



Title	A small secreted protein from <i>Zymoseptoria tritici</i> interacts with a wheat E3 ubiquitin to promote disease
Authors(s)	Karki, Sujit Jung, Reilly, Aisling, Zhou, Binbin, Mascarello, Maurizio, Burke, James, Doohan, Fiona M., Douchkov, Dimitar, Schweizer, Patrick, Feechan, Angela
Publication date	2021-02-02
Publication information	Karki, Sujit Jung, Aisling Reilly, Binbin Zhou, Maurizio Mascarello, James Burke, Fiona M. Doohan, Dimitar Douchkov, Patrick Schweizer, and Angela Feechan. "A Small Secreted Protein from <i>Zymoseptoria Tritici</i> Interacts with a Wheat E3 Ubiquitin to Promote Disease." Oxford University Press, February 2, 2021. https://doi.org/10.1093/jxb/eraa489 .
Publisher	Oxford University Press
Item record/more information	http://hdl.handle.net/10197/12757
Publisher's statement	This is an Open Access article distributed under the terms of the Creative Commons Attribution License (http://creativecommons.org/licenses/by/4.0/), which permits unrestricted reuse, distribution, and reproduction in any medium, provided the original work is properly cited.
Publisher's version (DOI)	10.1093/jxb/eraa489

Downloaded 2026-05-01 23:34:45

The UCD community has made this article openly available. Please share how this access benefits you. Your story matters! (@ucd_oa)



© Some rights reserved. For more information

A small secreted protein from *Zymoseptoria tritici* interacts with a wheat E3 ubiquitin to promote disease

Sujit Jung Karki¹, Aisling Reilly¹, Binbin Zhou², Maurizio Mascarello^{1,4}, James Burke¹, Fiona Doohan², Dimitar Douchkov³, Patrick Schweizer³□ and Angela Feechan¹

¹ *School of Agriculture & Food Science and UCD Earth Institute, University College Dublin, Belfield, Dublin 4, Ireland*

² *School of Biology and Environmental Science and UCD Earth Institute, University College Dublin, Belfield, Dublin 4, Ireland*

³ *Institute of Plant Genetics and Crop Plant Research (IPK), Cytogenetics, Gatersleben, D-06466, Germany*

⁴ *Ecology, Evolution and Biodiversity Conservation, Charles Deberiotstraat 8 32, 3000 Leuven, Belgium.*

□ In memory of Patrick (author deceased).

Author e-mail addresses:

sujit.karki@ucd.ie

aisling.reilly.2@ucdconnect.ie

binbin.zhou@ucd.ie

maurizio.mascarello@plantentuinmeise.be

Jimmy.Burke@ucd.ie

douchkov@ipk-gatersleben.de

schweiz@ipk-gatersleben.de

fiona.doohan@ucd.ie

angela.feechan@ucd.ie

Corresponding Author: Angela Feechan

angela.feechan@ucd.ie

1 **ABSTRACT**

2 Septoria Tritici Blotch, caused by the ascomycete fungus *Zymoseptoria tritici*, is a
3 major threat to wheat production worldwide. The *Z. tritici* genome encodes many
4 small, secreted proteins (*ZtSSP*) that likely play a key role in the successful
5 colonisation of host tissues. However, few of these *ZtSSPs* have been functionally
6 characterised for their role during infection. In this study, we identified and
7 characterised a small, conserved cysteine-rich secreted effector from *Zymoseptoria*
8 *tritici* which has homologues in other plant pathogens in the dothideomycetes.
9 *ZtSSP2* was expressed throughout *Z. tritici* infection in wheat with the highest levels
10 observed early during infection. A yeast two-hybrid assay revealed an interaction
11 between *ZtSSP2* and wheat E3 ubiquitin ligase in yeast and this was further
12 confirmed *in planta* using bimolecular fluorescence complementation, and co-
13 immunoprecipitation. Down-regulation of this wheat E3 ligase using virus-induced
14 gene silencing, increased the susceptibility of wheat to Septoria tritici blotch (STB).
15 Together these results suggest that TaE3UBQ likely plays a role in plant immunity to
16 defend against *Z. tritici*.

17

18

19

20

21

22

23

24

25

26

27

28 **Key words:** *Zymoseptoria tritici*, fungal pathogen, disease, wheat, E3 ubiquitin
29 ligase, effector

30 INTRODUCTION

31 Plant innate immunity includes the recognition of broadly conserved pathogen-
32 associated molecular patterns (PAMPs), for example fungal chitin, by plant pattern
33 recognition receptors (PRRs). This recognition initiates PAMP-triggered immunity
34 (PTI) to mount a primary defence (Jones and Dangl, 2006). Pathogen effector
35 proteins have evolved to bypass the initial defence response (PTI) resulting in a
36 scenario termed Effector Triggered Susceptibility (ETS). These proteins are typically
37 small, cysteine rich secreted proteins, and are known to manipulate host physiology
38 and interfere with plant immunity (Dou and Zhou, 2012). In return, plants possess
39 Resistance (R) genes which, upon recognition of pathogen effectors, activate
40 Effector Triggered Immunity (ETI) (Jones and Dangl, 2006; Deslandes and Rivas,
41 2012).

42 *Septoria tritici* blotch (STB) caused by *Zymoseptoria tritici* is one of the most
43 prevalent and economically devastating diseases in wheat-growing areas worldwide
44 (Eyal *et al.*, 1985; Fones and Gurr, 2015). As with other fungal pathogens, *Z. tritici* is
45 known to produce a series of small, secreted effector proteins (SSPs) throughout its
46 colonisation of wheat (do Amaral *et al.*, 2012; Mirzadi Gohari *et al.*, 2015; Rudd *et al.*,
47 2015). Only a handful of *Z. tritici* effectors have been characterised for their role
48 in pathogenesis: *Mg3LysM* and *Mg1LysM* are lysin motif containing effectors that
49 play an important role during the initial symptomless period of *Z. tritici* infection
50 (Marshall *et al.*, 2011). *Mg3LysM* competes with host chitin receptors by binding
51 fungal chitin fragments (Lee *et al.*, 2014). Another *Z. tritici* effector, MgNLP, belongs
52 to the Necrosis and Ethylene-Inducing Peptide 1 (NEP1)-like (NLP) family of
53 proteins. It can induce cell death in *Arabidopsis*, but not in wheat (Motteram *et al.*,
54 2009). In addition, *Z. tritici* secretes two necrosis inducing protein effectors (ZtNIP1
55 and ZtNIP2) that induce cell death and chlorosis in some wheat cultivars (M' Berek
56 *et al.*, 2015).

57 Recently, several *Z. tritici* candidate effectors were found to induce a cell death
58 phenotype when expressed in the non-host plant *Nicotiana benthamiana* (Kettles *et al.*,
59 2017). One of these candidate effectors was subsequently identified as a novel
60 fungal PAMP, termed Cell Death-Inducing 1 (ZtCDI1) (Franco-Orozco *et al.*, 2017).

61 Similarly, another candidate (Zt-6) was characterized as a secreted ribonuclease
62 which possess cytotoxic activity against other microbes as well as plants (Kettles *et*
63 *al.*, 2018). Additionally, avirulence effectors, namely AvrStb6 (Kema *et al.*, 2018;
64 Zhong *et al.*, 2017) and Avr3D1 (Meile *et al.*, 2018), are known to be recognized by
65 specific wheat cultivars. Recently, *Z. tritici* small, secreted proteins were found to
66 interact with wheat Septoria Responsive Taxonomically Restricted Genes namely,
67 TaSRTRG6 and TaSRTRG7 implicated in STB disease (Brennan *et al.*, 2020).
68 However, the function of these TRGs is unknown. While some *Z. tritici* candidate
69 effectors have been identified, the molecular targets in wheat and their role during
70 infection remain largely unknown. Therefore, there is a need to identify the wheat
71 host proteins targeted by these *Z. tritici* effectors.

72 In this study, we selected a conserved effector candidate (ZtSSP2) similarly
73 expressed in three different *Z. tritici* isolates. ZtSSP2 is a small, secreted protein
74 (22KDa) with ten cysteine residues that appears to be conserved within *Z. tritici*
75 isolates and other dothideomycete fungus. Furthermore, we showed that ZtSSP2
76 physically interacts with wheat E3 ubiquitin ligase (*TaE3UBQ*) and that virus-induced
77 gene silencing (VIGS) of TaE3UBQ resulted in increased *Z. tritici* susceptibility. This
78 study provides insights in to how a *Zymoseptoria tritici* effector likely targets a host
79 ubiquitin system to aid successful colonization.

80

81

82

83

84

85

86

87

88

89

MATERIALS AND METHODS

90

91

92 **Plant material, fungal strains, and growth conditions.**

93 *Nicotiana benthamiana* and wheat (*Triticum aestivum*) cv. Remus, Kanzler and
94 Longbow were used in this study. The cv. Remus and cv. Kanzler are moderately
95 susceptible to *Z. tritici* (Váry *et al.*, 2015; Brady, 1983) while cv. Longbow is
96 susceptible to *Z. tritici* (Brading *et al.*, 2002). *N. benthamiana* plants were grown
97 growth chambers at 16-hour light at 22°C / 8-hour dark at 18°C with 7500-8200 lux,
98 RH 70% ± 5% throughout the experiments and 4-6-week *N. benthamiana* plants
99 were used for localisation studies.

100 Wheat seeds (cv. Remus, cv. Longbow) were surface-sterilised and incubated for 3
101 days at 4°C for seed stratification and then incubated for 4 days at room temperature
102 without illumination to allow germination. Germinated seeds were transferred into
103 plastic pots containing John Innes Compost No. 2 (Westland Horticulture, UK) and
104 grown in a growth chamber at 16 hours day/8-hour night photoperiod at 13,000 lux,
105 RH 80% ± 5% at 19°C/12°C. For biolistic studies, wheat cv. Kanzler seedlings were
106 grown in a growth chamber at 16 hours day/8-hour night photoperiod at 15,000 lux,
107 RH 60% ± 5% at 20°C in pots containing IPK soil substrate.

108 The *Z. tritici* isolate IPO323 (Kema and van Silfhout, 1997), Irish isolates 560.11
109 (Lynch *et al.*, 2016) and 553.11 were used to infect the susceptible wheat cv. Remus
110 and Longbow. Both 560.11 and 553.11 were isolated from the wheat cv. Alchemy in
111 2011 from South Wexford, Ireland (S. Kildea pers. comm). Prior to use, isolates were
112 cultured on potato dextrose agar (PDA) and grown at 20°C for approximately 5-7
113 days. Fourteen-day old wheat seedlings were used for inoculation. For the disease
114 assay we used 10⁶ cfu/ml spore suspension as inoculum (Fones *et al.*, 2017; Shetty
115 *et al.*, 2003; Zhong *et al.*, 2017) to assess pycnidia and necrosis coverage following
116 VIGS of TaE3UBQ. Fungal spores from PDA cultures were harvested and spore
117 concentration was adjusted to 1 x 10⁶ ml⁻¹ in water containing 0.02% Tween 20.
118 Spore suspensions (5 ml per plant) were sprayed to runoff (5 ml) per wheat plant
119 using hand-held spray bottles. Control plants were sprayed with 5 ml of 0.02%
120 Tween 20 solution. Inoculated plants were covered with polythene bags to ensure
121 high humidity and removed after 72 h.

122 **Effector candidate selection**

123 The publicly available secretome dataset from do Amaral *et al.*, 2012 which is based
124 on the IPO323 reference genome (Goodwin *et al.*, 2011), was mined to identify *Z.*
125 *tritici* small, secreted proteins (*ZtSSPs*). 262 candidate genes with EST support were
126 screened based on small size (50 to 315 amino acids), resulting in 102 SSP's. These
127 were sorted based on the number of cysteine residues which resulted in 90 SSP's
128 with multiple cysteines (Fig. S1). The amino acid sequence was then used to predict
129 effector properties and any apoplastic localisation using EffectorP & ApoplasticP
130 (Table S1) (Sperschneider *et al.*, 2016, 2018). These were analysed using NCBI
131 CDD (Conserved Domain database) to update the prediction of any conserved
132 domains. Candidate effector proteins were analysed using BLASTP (cut-off value \geq
133 50% Identity and e-value ≤ 0.01) to search for homologues in other plant pathogenic
134 fungal species (Table S2). Finally, those that were unannotated (Table S1) and with
135 a potential homologue in other plant pathogenic fungi were selected. Of these, 17
136 non-annotated *ZtSSPs* were analysed for expression among three *Z. tritici* isolates
137 (IPO323, 553.11 and 560.11) at 7dpi. (Table S3). *Mycgr3G105265* (*ZtSSP2*) was
138 selected for further study based on these criteria and the similar expression levels
139 across all three isolates.

140

141 **Transcriptomics analysis**

142 Leaves (cv. Longbow) infected with the *Z. tritici* isolates IPO323, 553.11 and 560.11
143 from four independent replicates were collected at 7 dpi. RNA from each sample was
144 extracted at room temperature using the RNeasy Plant Mini Kit (QIAGEN), purified
145 from DNA contamination using DNase I (Sigma Aldrich) and stored at 20 °C. RNA
146 quality control was assessed by Agilent 2100 bioanalyzer. RNA was extracted from
147 two leaves from each of two seedlings infected with each isolate over four
148 independent experiments (n = 16), pooled and sent for RNA sequencing on an
149 Illumina HiSeq 2000 (paired-end 100 bp reads) at the 250 Beijing Genome Institute
150 (BGI) (Hong Kong).

151 Expression analysis was performed by General Bioinformatics (Reading, UK). The
152 reference genome for *Z. tritici* was from the MG2 assembly from ENSEMBL Fungi
153 release. The reference genome for *Triticum aestivum* was from the IWGSC1+popseq

154 assembly from ENSEMBL Plants release. The quality control of raw reads was
155 assessed with FastQC v0.11.5 (Andrews, 2010). Reads were trimmed to remove
156 contaminating adapter sequences and poor-quality bases at the beginning of the
157 reads using Trimomatic (Bolger *et al.*, 2014). Clean reads generated were
158 185,725,832 for IPO323 isolate infected leaf samples, 187,073,058 for 553.11 isolate
159 infected leaf samples and 183,036,662 for the 560.11 isolate infected leaf sample.
160 Unfiltered reads were aligned to the *Z. tritici* genome using Tophat v2.1.1 aligner
161 (Kim *et al.*, 2013). BAM files for reads mapped to the *Z. tritici* genome were
162 converted to SAM files and sorted for further analysis using Samtools v 1.3 (Li *et al.*,
163 2009). Then, reads were counted using the htseq-count script of the HTSeq v 0.6.0
164 (Anders *et al.*, 2015). Fragments Per Kilobase of transcript per Million mapped reads
165 (FPKM) values for each sample were calculated using Cufflink package (Trapnell *et*
166 *al.*, 2010). Genes with a total read count lower than 1 were filtered out. Counts were
167 normalised using TMM (Robinson *et al.*, 2010) and the common dispersion BCV
168 (square-root-dispersion) was set at 0.4. Pairwise comparison between datasets were
169 made using the exact test (Robinson *et al.*, 2008). Filtered reads were aligned to the
170 *T. aestivum* genome using Tophat v2.1.1. The BAM file containing the unmapped
171 reads was converted back to FastQ format using the bam2fastx utility of Tophat (Kim
172 *et al.*, 2013). The alignment to the *Z. tritici* genome and subsequent analysis were
173 performed as described for the unfiltered reads.

174

175 **Amplification and Cloning of ZtSSP2**

176 ZtSSP2 was amplified from wheat (cv. Remus) infected with *Z tritici* isolate 560.11 c-
177 DNA with and without the signal peptide using Phusion High Fidelity Polymerase
178 (New England Biolabs) and primers flanked with gateway adapter sequence (Table
179 S4). AttB-flanked PCR products were purified using QIA quick PCR Purification Kit
180 (Qiagen) and cloned into pDONR207 (Invitrogen) using BP clonase II enzyme mix
181 (Thermo Fisher Scientific) and subsequently cloned into the binary vector
182 pEARLYGATE 101 (pEG101) (Earley *et al.*, 2006) using LR clonase II enzyme. Entry
183 clones were sequence verified by sequencing (Macrogen Europe) before LR
184 reaction. All other destination vectors are described separately.

185

186 **Validation of protein secretion using a yeast sucrose secretion system**

187 A gateway compatible vector (pGADT7) for yeast secretion assay and *suc2* yeast
188 mutant (strain SEY6210) was utilised (Brennan *et al.*, 2020). Briefly, the invertase
189 (*SUC2*) gene with and without signal peptide was amplified from the yeast strain
190 BY4741 with a linker (Kex2 site) added between the gateway reading frame and
191 *SUC2* gene. This construct was ligated into pGADT7 vector and verified by
192 sequencing. Candidate *ZtSSP2* and ΔSP -*ZtSSP2* was cloned into the yeast
193 secretion vector in frame with N terminus of *SUC* gene and transformed into *suc2*
194 yeast mutant. Transformants were PCR validated and selected on a synthetic
195 dropout medium (minus Trp and leu) with sucrose as a sole carbon source. Yeast
196 spotting was performed with dilution of 10^{-1} , 10^{-2} and 10^{-3} respectively. The
197 experiment was repeated three times independently with three replicates per
198 experiment.

199

200 **Phylogenetic analysis of ZtSSP2**

201 BLASTp search was performed using the NCBI (National Centre for Biotechnology
202 Information) BLAST service (<http://blast.ncbi.nlm.nih.gov/Blast.cgi>) and uniprot blast
203 (<http://www.uniprot.org/blast/>). Sequences of the 20 closest homologues of ZtSSP2
204 (Table S5) were aligned using ClustalW, and a phylogenetic tree was constructed
205 using the maximum likelihood (ML) method with 1000 bootstrap replicates in Mega7
206 (Kumar *et al.*, 2016).

207

208 **RNA extraction and quantitative RT-PCR**

209 100 mg of infected leaves (cv. Remus) per sample was collected at different days
210 post infection (dpi), frozen in liquid nitrogen and stored at -80 °C. Total RNA was
211 extracted from *Z. tritici* infected wheat leaves using the RNeasy Mini Kit (Qiagen)
212 following the manufacturer's instructions. RNA was then subjected to on-column
213 DNase treatment (Sigma). Quantification of total RNA was carried out using a
214 Nanodrop ND-1000 spectrophotometer. Reverse transcription of 1-2µg RNA for
215 cDNA synthesis was carried out using Omniscript RT Kit (Qiagen).

216 Real-Time quantitative PCR was carried out in 12.5 µl reactions including 1.25 µl of
217 a 1:5 (v/v) dilution of cDNA, 0.2 µM of primers, and 1× SYBR Premix Ex Taq (Tli
218 RNase H plus, RR420A; Takara). PCR conditions were as follows: 1 cycle of 1 min
219 at 95°C; 40 cycles of 5 s at 95°C and 20 s at 60°C; and a final cycle of 1 min at
220 95°C, 30s, at 55°C, and 30 s at 95°C for the dissociation curve. For *ZtSSP2*
221 expression, RNA was extracted from the 3rd leaf of wheat seedlings and from three
222 individual leaves from different seedlings per time point per replicate. Three
223 independent experiments were performed. qPCR was performed using QuantStudio
224 7 Flex Real-Time PCR system (Applied Biosystems) and the relative gene
225 expression was calculated as $2^{-(Ct \text{ target gene} - Ct \text{ housekeeping gene})}$ as previously described
226 (Livak and Schmittgen, 2001). *Z. tritici tubulin* was used as housekeeping gene
227 control for the *ZtSSP2* time course. While for VIGS, Ct housekeeping gene =
228 geometric mean (Ct *Tacdc48*: Ct *Taelf4E*) of two wheat reference genes; Cell
229 division control protein 48 (*TaCDC48*) and Eukaryotic Initiation factor 4E (*TaeIF4E*)
230 (Lee *et al.*, 2014).

231

232 **Single-cell death assay in wheat**

233 The cell death assay in wheat was performed as previously described (Pliego *et al.*,
234 2013). Briefly, seven leaves of 7-day old wheat (approx. 8 cm in length) cv. Kanzler
235 was co-bombarded (PDS-1000/He System, Bio-Rad) with 7µg of pEG101: (ΔSP)
236 *ZtSSP2* (over-expression), 7µg pUbiGUS (β-glucuronidase reporter for
237 transformation efficiency) and 7µg of the *B-Peru/C1*-expression plasmid pBC17
238 (Schweizer *et al.*, 2000) for inducing anthocyanin production (as a marker for live
239 cells). Four days post bombardment, cells accumulating anthocyanin were counted
240 and leaves were then stained with 5-bromo-4-chloro-3-indolyl glucuronide (X-gluc)
241 solution overnight at 37°C. Leaves were destained with trichloroacetic acid
242 (Douchkov *et al.*, 2005). The number of cells with visible GUS stain was counted and
243 the relative number of anthocyanin producing cells was calculated as the ratio of
244 anthocyanin accumulated cells to the number of β-glucuronidase (GUS) expressing
245 cells. The experiment was repeated four times independently and seven leaves
246 counted per replicate.

247

248 **Yeast two-hybrid analysis**

249 The c-DNA library was comprised of leaf three of wheat seedlings cv. Stigg and
250 Longbow which were infected with a mixture of *Z. tritici* isolates (IPO323, 560.11 and
251 Cork cordiale 4) (Brennan *et al.*, 2020; Kema *et al.*, 1997; Lynch *et al.*, 2016),
252 collected at various time points (1, 2, 4, 6, 8, 10, 12 dpi) then pooled together for
253 RNA extraction. Briefly, the c-DNA of (Δ SP) *ZtSSP2* was cloned into pB27 vector as
254 an N-LexA-bait-C fusion to LexA. The construct encoding *ZtSSP2* was used as bait
255 to screen the c-DNA library of wheat leaves inoculated with *Z. tritici*.

256 The initial yeast two-hybrid screening was performed by Hybrigenics Services,
257 S.A.S. (<http://www.hybrigenics-services.com>). A total of 76.4 million clones were
258 screened and 73 positive clones were processed following selection on selective
259 medium lacking Trp, Leu, and His supplemented with 0.5mM 3AT. The prey
260 fragments from positive clones were amplified and sequenced. The putative high
261 confidence interactors are listed in Table S6. These sequences were used to identify
262 corresponding proteins in the NCBI GenBank database including TaE3UBQ. For
263 analysis of a specific interaction, CDS of *TaE3UBQ*, *TaE3UBQ*₁₂₆₋₂₁₉, barley
264 homologue of E3UBQ; HvUBQ and (Δ SP) *ZtSSP2* and the *Ramularia collo-cygni*
265 homologue of *ZtSSP2*; RcSSP2 was cloned into the vector pDONR207 using
266 Gateway cloning technology. They were then recombined into bait and prey vectors
267 derived from pGADT7 and pGBKT7 plasmids (Clontech, USA). Analysis of protein-
268 protein interactions was performed using the Gal4 two-hybrid assay as described in
269 Perochon *et al.*, 2010. As a negative control to ensure specific interactions with
270 *ZtSSP2*, another small secreted effector candidate (Δ SP) *Zt-10* was used (Kettles *et*
271 *al.*, 2017) while the positive control included TaSSP6 and *Zt-06* (Zhou *et al.*, 2020).

272

273 **Agrobacterium mediated transient expression**

274 *A. tumefaciens* strain GV3101 was transformed by electroporation with effector
275 constructs and grown for 48 hrs at 28°C 220rpm in LB medium with the antibiotic
276 gentamicin (25mg/ml) and kanamycin (50mg/ml). Transformed cells were harvested
277 by centrifugation and suspended in infiltration buffer (10mM MgCl₂, 10mM 2-(N-
278 mopholino) ethanesulfonic acid (MES) pH 5.6 and acetosyringone 150µM) at an

279 absorbance 600nm (OD_{600}) of 0.5. The bacterial suspension was left at room
280 temperature for 2hr before infiltration into 4-6-week-old *N. benthamiana* on the
281 abaxial side of the leaves using a 1ml needleless syringe.

282

283 ***In planta* validation of protein-protein interaction**

284 For *in planta* analysis of the interaction between (Δ SP) ZtSSP2 and TaE3UBQ the
285 coding sequences were cloned in the gateway vector pDONR207 (Invitrogen, USA)
286 and subsequently cloned into the bimolecular fluorescence complementation (BiFC)
287 vectors pDEST-GW VYCE, pDEST-VYCE GW, pDEST-GW VYNE and pDEST-
288 VYNE GW (Gehl *et al.*, 2009). This resulted in constructs where proteins were fused
289 at either the N or C terminal to the YFP C-terminal (YFP^C) or N-terminal fragment
290 (YFP^N). For localisation of TaE3UBQ, LR reaction was performed with pGWB406
291 (Nakagawa *et al.*, 2007). Vectors were transformed into *A. tumefaciens* strain
292 GV3101 by electroporation. Transformants containing the plasmids were selected on
293 LB agar plates containing 10 μgml^{-1} rifampicin, 20 μgml^{-1} gentamicin and 50 μgml^{-1}
294 kanamycin. A mix of Agrobacterium transformants was prepared: $OD_{600} = 0.5$ and
295 0.5 and 0.1 of YFPC construct, YFPN and P19 silencing construct, respectively. This
296 mix was syringe-infiltrated into leaf epidermal cells of 3-4-week-old *N. benthamiana*,
297 by making a small injury into the leaf and pressure infiltrating. For TaE3UBQ
298 localisation, MG132 (100 μm) was infiltrated into leaves for 6h before analysis to
299 prevent protein degradation. Images were analysed using a confocal laser scanning
300 microscope (Olympus fluoview FV1000). GFP and YFP excitation was performed at
301 515 nm and emission detected in 530 to 630 nm range. These experiments were
302 repeated at least twice independently, and each experiment included three leaves,
303 each from an individual plant.

304

305 **Co-immunoprecipitation (Co-IP) Assay**

306 The protein construct was transiently overexpressed in *N. benthamiana* leaves using
307 agro-infiltration. Leaf samples were collected at 48hr post infiltration, TaE3UBQ and
308 GFP samples were infiltrated with MG132 (100 μm) 6h before collection. Proteins
309 were extracted using GTEN buffer (25 mM Tris-HCl pH 7.5, 150 mM NaCl, 1 mM

310 EDTA, 10% glycerol 0.1% Tween 20) with 2% W/V polyvinylpolypyrrolidone (PVPP),
311 10 mM dithiothreitol (DTT), and a protease inhibitor cocktail (Sigma). Samples were
312 incubated for 15 min in lysis buffer (4°C). Lysate was centrifuged at 10,000g for 10
313 min and 250 µl of supernatant subjected to Co-IP with GFP-Trap®-M magnetic
314 beads (Chromotek, Germany) for affinity binding of GFP-fused proteins at 4°C for 4
315 hours. The beads were washed three times with 500 µl of extraction buffer. Protein
316 bound to magnetic beads was boiled for 10 min for elution. Eluted proteins and crude
317 proteins (input) were detected by western blotting. Immunoblotting of the proteins on
318 the PVDF membrane were detected using the corresponding anti-HA (1:1000;
319 Roche) and anti-GFP (1:5000; Invitrogen) antibody.

320

321 **BSMV mediated gene silencing (VIGS)**

322 The barley stripe mosaic virus (BSMV)-derived VIGS vectors used in this study
323 consisted of the wild type BSMV ND18 α , β , γ tripartite genome (Holzberg *et al.*,
324 2002; Scofield *et al.*, 2005). A BSMV γ vector construct containing a 185 bp-
325 fragment of the barley phytoene desaturase gene (BSMV: PDS) was used as
326 positive control for VIGS, as previously described (Scofield *et al.*, 2005) (Fig. S2).
327 Two independent, non-overlapping gene constructs (UBQV1 and UBQV2) were used
328 for gene silencing (Fig. S3). Both gene fragments were PCR-amplified and chosen to
329 target *TaE3UBQ-1D* and its homoalleles (*TaE3UBQ-1A* and *TaE3UBQ-1B*). The
330 specificity and silencing efficiency were evaluated by BLASTn and using SGN VIGS
331 tool with *T. aestivum IWGSC2* as a database (Fernandez-Pozo *et al.*, 2015). PCR-
332 amplified fragments were ligated in the antisense orientation into *NotI/Pac1*-digested
333 BSMV γ vector pSL038-1 (Scofield *et al.*, 2005). Construct authenticity was verified
334 by sequencing.

335 Vectors containing the BSMV α , γ genomes and the γ genome vectors containing
336 either BSMV: UBQV1, BSMV: UBQV2, or BSMV: PDS were linearized with *MluI*. The
337 BSMV β genome was linearized with *SpeI*. Capped *in vitro* transcripts were prepared
338 from the linearized plasmids using the mMessage mMachine T7 in vitro transcription
339 kit (AM1344, Ambion) following the manufacturer's protocol. RNA quantity and
340 quality were evaluated using the ND-1000 spectrophotometer (NanoDrop, Thermo
341 Fisher Scientific, United States) measurement. Capped BSMV transcripts (1:1:1)

342 with 1X FES buffer were rub-inoculated onto the second leaf of the two-leaf stage of
343 the wheat cultivar Longbow. BSMV: PDS was used as positive control, whereas
344 BSMV γ and 1X FES buffer was used as negative control. Fourteen days after virus
345 inoculation, the third and fourth leaves of virus inoculated wheat seedlings (12 plants
346 per treatment per trial) were infected with *Z. tritici* (560.11). The third leaves were
347 collected at 10 dpi and RNA extracted individually from each of the leaves per
348 treatment. The fourth leaves were used for STB disease symptom phenotyping at 21
349 days post inoculation (10 leaves per treatment, 3 independent trials). Seven leaves
350 per treatment per replicate were submerged in 10 ml deionised water for 1 hour and
351 vortexed to collect spores and 10 μ l counted using a haemocytometer.

352

353 **Statistical Analysis**

354 Statistical analysis of the data was carried out using the R statistical software (R
355 Core Team, 2016). All data from the studies were checked for normal distribution
356 and when necessary, variances were stabilized using Box-cox transformation. A
357 generalised linear model was used to test the data and significant differences were
358 determined using the Tukey test at $P < 0.05$. For analysis of VIGS data (phenotyping
359 and spore counts), data were fitted to a generalised linear mixed model with binomial
360 distribution to account for over-dispersion and zero-inflation. Significance of
361 differences between treatments was assessed using the Tukey's HSD.

362

363

364

365

366

367

368

369

370

372 **1. ZtSSP2 is a conserved small, secreted protein candidate**

373 The publicly available secretome dataset from do Amaral *et al.*, 2012 was mined to
374 identify *Z. tritici* small, secreted proteins (*ZtSSPs*). 262 candidate genes with
375 expressed sequence tag (EST) support were screened based on small size (50 to
376 315 amino acids) resulting in 102 *ZtSSPs*. These proteins were then sorted based
377 on number of cysteine residues (≥ 1) which resulted in 90 *ZtSSPs* (Fig. S1). The
378 amino acid sequence was then used to predict effector properties and any apoplastic
379 localisation using EffectorP & ApoplasticP (Table S1). Further analysis of these
380 candidates showed that 52% were predicted to be effector proteins while, 81% were
381 predicted to be apoplastic proteins (Table S1) (Sperschneider *et al.*, 2016, 2018).
382 The 90 candidate effector proteins were analysed using BLASTP (cut off value as \geq
383 50% identity and E-value ≤ 0.01) to search for homologues. Fifty-nine of these
384 *ZtSSP* candidates had a homologue in another plant-pathogenic fungal species
385 (Table S2 and S7). Of the fifty-nine *ZtSSPs* thirteen were found to have a homologue
386 in *Zymoseptoria brevis* only (Table S7). Forty-three *ZtSSPs* had a homologue in in *Z.*
387 *brevis* as well as another plant pathogen while three had a homologue in a different
388 plant pathogenic species other than *Z. brevis* (Table S2). Of the forty-three,
389 seventeen were non-annotated proteins and twenty-six candidates had annotated
390 protein domains. We examined the expression of these seventeen conserved non-
391 annotated effector candidates across three *Z. tritici* isolates at 7 dpi. The expression
392 of *Mycgr3G105265* (*ZtSSP2*) was similar (FKPM 148, 126 and 177) across all three
393 isolates (IPO323, 553.11 and 560.11 respectively) compared to other *ZtSSP*
394 candidates (Table S3). We selected the effector candidate *ZtSSP2* for functional
395 characterisation as we reasoned that the conservation across different plant
396 pathogenic species (Table S2:S5) and the similar levels of expression across three
397 different *Z. tritici* isolates (Table S3) may indicate a conserved core effector.
398 *ZtSSP2* is predicted to have an N-terminus signal peptide (0.9986 likelihood,
399 SignalP4.1) (Nielsen *et al.*, 2017). To validate this, we tested the secretion of
400 *ZtSSP2* using a yeast secretion assay (Fig 1a; Brennan *et al.*, 2020). The full length
401 *ZtSSP2* protein could complement the *suc2* knock out yeast strain allowing it to grow

402 in selection media containing sucrose as a sole source of carbon (Fig. 1b). These
403 characteristics suggest ZtSSP2 is a conserved secreted effector protein.

404

405 **2. Homologues of ZtSSP2 are conserved in the Dothideomycete fungi.**

406 For ZtSSP2 we found additional potential homologues in other dothideomycetes. All
407 the potential homologues of ZtSSP2 identified within the plant pathogenic
408 *Mycosphaerellaceae* family were of similar size, possessed an N-terminal signal
409 peptide and contained ten conserved cysteine residues (Fig. 2a). For example, the
410 homologue from the conifer infecting fungi *Dothistroma septosporum* shares 53.57%
411 sequence similarity, that from the barley pathogen *Ramularia collo-cygni* is 51.67%
412 identical to ZtSSP2, and that from the banana pathogen *Mycosphaerella fijiensis*
413 shares 51% sequence identity. The majority of homologues (13) were from plant
414 pathogens but other homologues were from two eurotiomycetes which are human
415 pathogens (Fig. 2b) (Table S5). There was also an outgroup of dothidoemycetes
416 which were non-pathogenic (Fig. 2b).

417

418 **3. ZtSSP expression during STB infection in wheat**

419 Pathogen effector genes are known to be induced transcriptionally during infection of
420 the host plant (Stergiopoulos and de Wit, 2009). We performed a quantitative
421 reverse transcription PCR (qRT-PCR) to determine the expression of ZtSSP2 during
422 infection. The *Z. tritici* isolate 560.11 (Lynch *et al.*, 2016) was used to infect wheat
423 (cv. Remus) and the expression of ZtSSP2 determined over 2, 4, 8, 10 dpi
424 (representing biotrophic stage), 14, 21 dpi (necrotrophic stage) compared to the
425 uninfected control (Fig. 3). Based on expression analysis, ZtSSP2 was expressed
426 from 2 dpi through to 21 dpi. The expression was significantly higher at 2 dpi
427 compared to all other time points suggesting potential role early in biotrophy. There
428 was a significant dip in expression at 14 dpi compared to 2 and 21 dpi (Fig.3).

429

430 **4. ZtSSP candidates did not induce cell death in wheat**

431 We used a transient leaf expression system by Pliego *et al.*, 2013, to assess whether
432 ZtSSP2 can induce cell death. In this system transient expression of the maize

433 transcription factor *B-Peru* and *C1* leads to accumulation of anthocyanin only in
434 intact vacuoles of viable cells and can therefore be used as a cell death marker
435 (Schweizer *et al.*, 2000). We co-bombarded pEG101: (Δ SP) *ZtSSP2* overexpression
436 construct with pUbiGUS (cell death insensitive transformation marker) and
437 anthocyanin expression plasmid pBC17 into wheat leaves. Co-bombardment of
438 pBC17 with pUbiGUS and the vector pEG101 was used as a negative control while,
439 *Zt-6* previously reported to induce cell death in wheat (Kettles *et al.*, 2018) was used
440 as a positive control, respectively. The number of cells accumulating anthocyanin
441 (Fig. 4a) was counted and then leaves were subsequently stained for GUS activity
442 (Fig. 4b). The number of cells stained with GUS was also counted. The ratio of
443 anthocyanin to GUS cells was used as an estimate of cell death. The empty vector
444 control (pEG101) resulted in the average ratio of 1.27 (Fig. 4c), while the positive
445 control (pEG101: *Zt-6*) showed a reduced ratio of 0.3 ($P < 0.05$). The anthocyanin to
446 GUS ratio obtained from bombardment of *ZtSSP2* was not significantly different from
447 the control suggesting no cell death activation by this effector candidate in wheat.

448

449 **5. Candidate *ZtSSP2* interacts with wheat ubiquitin ligase *in vitro* and *in planta***

450 We performed a yeast two-hybrid screen to determine if *ZtSSP2* could interact with
451 wheat host components. A cDNA expression library generated from *Z. tritici* infected
452 wheat leaves was screened using *ZtSSP2* as bait. A wheat cDNA clone encoding
453 the extracellular region (amino acids 126-219) of a C3H2C3-type RING E3 ubiquitin
454 ligase protein (TaE3UBQ) was identified. Pathogen effectors have been reported to
455 target the host ubiquitin system to manipulate host defence (Park *et al.* 2012). To
456 investigate if *ZtSSP2* interacts with the wheat E3 ligase (TaE3UBQ) and thereby
457 manipulates the wheat host ubiquitin proteasome system this protein-protein
458 interaction was tested in yeast (*Saccharomyces cerevisiae*) using a galactose-
459 responsive transcription factor GAL4-based yeast two-hybrid system (Fig. 5a). We
460 cloned TaE3UBQ and TaE3UBQ₁₂₆₋₂₁₉ from wheat cDNA and found that
461 (Δ SP)*ZtSSP2* interacted with TaE3UBQ₁₂₆₋₂₁₉ but not with the full-length protein in
462 yeast (Fig. 5a). TaE3UBQ homologue HvE3UBQ was found in barley, and the
463 *ZtSSP2* homologue RcSSP2 found in the barley pathogen *Ramularia collo-cygni*
464 (Fig. 6). Therefore, this interaction was also tested (Fig. S4). However, no positive

465 interaction between (Δ SP)RcSSP2 and Hve3UBQ was observed. When RcSSP2
466 was replaced with (Δ SP)ZtSSP2 we found that Hve3UBQ₁₂₆₋₂₁₉ also interacts with
467 ZtSSP2 in yeast (Fig. S4).

468 Additionally, the interaction between (Δ SP)ZtSSP2 and TaE3UBQ was
469 investigated *in planta* using the BiFC system (Gehl *et al.*, 2009). TaE3UBQ and
470 (Δ SP)ZtSSP2 were fused at the N terminus and C-terminus of YFP respectively. The
471 resulting constructs were co-expressed using *Agrobacterium* infiltration in *N.*
472 *benthamiana* leaves. A strong YFP signal was observed, when YFP^N-TaE3UBQ
473 was co-infiltrated with YFP^C- (Δ SP)ZtSSP2 (Fig. 5b). To test if the interaction of
474 TaE3UBQ was specific to ZtSSP2, co-infiltration with another putative *Z. tritici*
475 effector; YFP^C- (Δ SP)Zt-10 was performed. No YFP fluorescence was observed with
476 this construct suggesting no interaction of TaE3UBQ with candidate (Δ SP)Zt-10.
477 Cnx6 homodimers were used as positive control (Gehl *et al.*, 2009).

478 We used co-immunoprecipitation (Co-IP) to further validate the interaction of
479 TaE3UBQ with ZtSSP2. The HA-tagged TaE3UBQ was co-expressed with a GFP
480 fusion of ZtSSP2 in *N. benthamiana* and subjected to Co-IP assay using GFP-
481 Trap®-M magnetic beads. Western blot analysis showed that only HA-tagged
482 TaE3UBQ was co-immunoprecipitated on GFP-Trap®-M beads and specifically
483 detected with the anti-HA antibody in presence of GFP-ZtSSP2, but not in the GFP
484 control (Fig. 5c). Taken together, these results reveal that ZtSSP2 interacts with
485 TaE3UBQ *in vitro* and *in planta*.

486

487 **6. Wheat ubiquitin represents is a C3H2C3 ring finger E3 protein ligase with a** 488 **transmembrane helix.**

489 The full-length cDNA of TaE3UBQ (TraesCS1D02G119700) was obtained by
490 comparing the clone sequence with EnsemblPlants IWGSC database. BLASTp
491 showed that TaE3UBQ has two additional homeologs in wheat namely:
492 TraesCS1A02G118800 and TraesCS1B02G138300 sharing 99.3 and 97% similarity
493 with its 1D variant respectively. The TaE3UBQ ORF encodes a RING finger protein
494 of 420 amino acids, with a theoretical pI value of 6.06 and a deduced molecular
495 mass of 46.2 kDa (Fig. 6a). Protein sequence analysis using NCBI CDD (Marchler-
496 Bauer *et al.*, 2017) and MemBrain 3.1 (Yin *et al.*, 2018) programs showed a C-

497 terminus C3H2C3 Zinc-finger domain with transmembrane helix and extracellular
498 loop region (Fig. 6a, 6b) (Fig. S5). Alignment of TaE3UBQ revealed that the RING
499 finger domain is conserved among various plant species (Fig. 6b). We performed
500 localisation of GFP-tagged TaE3UBQ in *N. benthamiana* leaves. The fluorescent
501 signal from *GFP-TaE3UBQ* was predominantly localised at the cell periphery similar
502 to the signal obtained by expression of a plasma membrane marker pm-yk (Nelson
503 *et al.*, 2007), whereas the GFP control was distributed throughout the cell including
504 the nucleus (Fig. 6c).

505

506 **7. Silencing *TaE3UBQ* enhances wheat susceptibility to *Z. tritici***

507 We examined the expression of *TaE3UBQ* homeologs using expVIP (expression
508 Visualization and Integration Platform) (Borrill *et al.*, 2016). All three wheat
509 homeologs have a similar expression profile and levels were not significantly
510 different between mock and *Z. tritici* treatment (Fig. S6). Virus-induced gene
511 silencing was used to determine the role of *TaE3UBQ* during the interaction of *Z.*
512 *tritici* with wheat (cv. Longbow) (Fig. 7). Two independent non-overlapping constructs
513 (UBQ_V1, UBQ_V2) were used to target all three *TaE3UBQ* homeologs (Fig. S3).

514 Expression of three homeologs was measured using a primer pair in a conserved
515 region (Fig. S3). qRT-PCR analysis of gene silenced leaf tissue (BSMV:UBQ_1 and
516 BSMV:UBQ_2) showed that, compared to the control (BSMV:00) plants, *TaE3UBQ*
517 expression (all homeologs) was significantly reduced by 53-70% in mock inoculated
518 leaves and 59-76% in *Z. tritici* inoculated leaves of the wheat cv. Longbow (Fig. 7a).
519 Silencing using construct UBQ_V1 showed higher efficiency than construct UBQ_V2.
520 Phenotypic assessment of wheat leaves at 21 days post *Z. tritici* infection revealed
521 that BSMV:UBQ_V1 and BSMV:UBQ_V2 leaves had significantly increased disease
522 coverage as represented with higher necrosis and pycnidia coverage compared to
523 control leaves (BSMV:00), (Fig. 7b,7c). This was reflected by the significantly higher
524 *Z. tritici* spore numbers found in BSMV: UBQ_V1 and BSMV: UBQ_V2 treated
525 leaves compared to the BSMV:00 control (Fig. 7d).

526

527

528

DISCUSSION

530 The major component of the filamentous plant pathogens secretome are often small,
531 secreted cysteine rich proteins (SSPs) (Stergiopoulos and de Wit, 2009). These
532 SSPs are small (300aa) with cysteine residues and a secretion signal at the N-
533 terminus. SSPs from plant pathogens play a key role in subverting host plant
534 immunity and facilitating colonisation (Hogenhout *et al.*, 2009; Rafiqi *et al.*, 2012).
535 Therefore, understanding how pathogen SSPs function in a host plant and the
536 potential host targets is key for complete understanding of molecular mechanism of
537 pathogenicity and disease.

538 In this study, we characterise a small secreted protein ZtSSP2, as an effector
539 candidate, from *Z. tritici* which is conserved across the dothideomycetes. Fungal
540 pathogen effectors are secreted in host, have diverse functions and are differentially
541 regulated throughout infection (Chen *et al.*, 2013). ZtSSP2 was functionally secreted
542 using a yeast secretion system suggesting it is a potential pathogen secreted
543 effector candidate protein (Fig. 1).

544 *Z. tritici* has a long latent/biotrophic phase prior to necrotrophy and has been
545 described as a hemibiotroph (Rudd *et al.*, 2015) or a latent necrotroph (Sánchez-
546 Vallet *et. al.*, 2015). During the latent phase which lasts for 7-10 days *Z. tritici* may be
547 endophytic (Sánchez-Vallet *et. al.*, 2015) or even epiphytic (Fones *et al.*, 2017).
548 ZtSSP2 expression levels were highest at 2 dpi during the latent/biotrophic phase of
549 the pathogen before dipping at 14 dpi following the switch to the necrotrophic phase
550 which takes place from around 10 dpi (Rudd *et al.*, 2015). A biphasic expression
551 pattern was also reported for ZtSSP2 previously (Mirzadi Gohari *et al.*, 2015).

552 To test a possible role for ZtSSP2 in cell death and potentially the necrotrophic
553 lifestyle of *Z. tritici*, we utilized a biolistic approach with an anthocyanin marker for
554 cell death in wheat. Our results showed that ZtSSP2 does not induce cell death in
555 wheat leaves. Ubiquitin E3 ligases can act as either positive or negative regulators
556 of plant immunity controlling the degradation of different protein substrates (McLellan
557 *et al.*, 2020). In rice the RING E3 ligases, APIP6 and APIP10 are positive regulators
558 of PTI as well as targets of the *Magnaporthe oryzae* effector AvirPiz-t. When either
559 APIP6 or APIP10 are silenced PTI is compromised including impaired reactive
560 oxygen species production and defence gene induction (Park *et al.*, 2016). The
561 reactive oxygen species, hydrogen peroxide is known to restrict *Z. tritici* growth

562 during the latent/biotrophic phase (Shetty *et al.*, 2003). It is conceivable that
563 TaE3UBQ plays a similar role in wheat positively regulating PTI. Overexpression of
564 *ZtSSP2 in planta* may promote interaction with TaE3UBQ and compromise PTI
565 which would not induce cell death in agreement with our results (Fig. 4). Silencing
566 TaE3UBQ would also compromise PTI. This is in line with the increased necrosis
567 and pycnidia formation observed with VIGS of TaE3UBQ (Fig. 7). Thus, ZtSSP2,
568 may interact with TaE3UBQ to compromise E3UBQ ligase activity, suppressing PTI.
569 ZtSSP2 has homologues in other members of the Dothideomycetes class, including
570 the pine infecting hemibiotroph *D. septosporum*, banana infecting *P. fijiensis*, and
571 barley pathogen *R. collo-cygni*. This broad conservation suggests that ZtSSP2 may
572 be a core effector candidate in dothideomycete pathogens. Of the homologous
573 proteins identified thirteen of these are from plant pathogens (Fig. 2b). We explored
574 a possible interaction between *R. collo-cygni*, RcSSP2 and barley Hve3UBQ.
575 However, we did not observe a strong interaction of RcSSP2 (homologue of ZtSSP2
576 with 51.67% similarity) with Hve3UBQ or Hve3UBQ₁₂₆₋₂₁₉ however, ZtSSP2 was
577 found to interact with Hve3UBQ₁₂₆₋₂₁₉ (Fig. S4) demonstrating this plant host target is
578 conserved. Homologues do also exist in two eurotiomycetes (*Cyphellophora*
579 *europaea* and *Fonsecaea monophora*, 40-45% homology) which can cause disease
580 in humans (de Hoog *et al.*, 2000; Queiróz *et al.*, 2018). In the outgroup of other
581 dothidoemycetes which are non-pathogenic (Fig. 2b) some of these have been
582 reported to be lichen forming fungi. Recently lichen forming fungi were reported to
583 express SSPs (Armaleo *et al.*, 2019).

584 A range of virulence effectors from plant pathogens concentrate into a limited
585 number of host cellular targets “Hubs” to subvert the host defence and enhance
586 virulence (Mukhtar *et al.*, 2011). One of the key regulatory networks in plant defence
587 is the ubiquitin-proteasome system (UPS). This UPS regulates multiple aspects of
588 plant immunity involving recognition, receptor protein accumulation and subsequent
589 defence signalling (Marino *et al.*, 2012; Ustun *et al.*, 2016). Therefore, manipulation
590 of host UPS by effectors is central to increasing pathogen virulence. Here, the *Z.*
591 *tritici* candidate effector ZtSSP2 was found to physically interact with a wheat host
592 E3 Ubiquitin ligase (*TaE3UBQ*) both in yeast and *in planta*. Domain analysis of
593 *TaE3UBQ* showed that it possesses a conserved RING-finger domain and four
594 transmembrane domains accompanied by an extracellular loop in the middle (Fig.

595 6a, S5). The localisation of *TaE3UBQ* in *N. benthamiana* leaves suggests that
596 *TaE3UBQ* could be localised predominantly to the cell periphery as a membrane
597 localised protein. RING-finger domains are characteristic of RING-class E3 ubiquitin
598 protein ligases that transfer ubiquitin from an E2 enzyme to a substrate protein. The
599 RING domain mediates the interaction with the appropriate E2 enzyme (Van Wijk *et al.*,
600 2009). These E3 ligases are central to plant immune responses and are also
601 known targets for pathogen secreted effector proteins. One such example was
602 effector *AvrPiz-t* from the blast fungus *M. oryzae*. *AvrPiz-t* has been shown to
603 interact and inhibit the rice RING-type E3 Ubiquitin ligase (APIP6) *in vitro* resulting in
604 the suppression of the APIP6 mediated PTI response (Park *et al.*, 2012). The
605 effector AVR3a from *P. infestans* interacts and stabilizes the host U-box E3 ligase
606 CMPG1 (Cys, Met, Pro and Gly protein 1) that is required for INF-1 triggered cell
607 death. The Avr3a interaction with CMPG1 leads to CMPG1 modification and thus
608 prevents host cell death induction during infection (Bos *et al.*, 2010).

609 In wheat we found three homoalleles of *E3UBQ* gene on chromosome 1DS,
610 1A and 1B and we hypothesize that all of them could be targets of ZtSSP2 as they
611 appear to be conserved (Fig. S6). For example, this was also observed for the stripe
612 rust effector PEC6 that interacts with wheat adenosine kinases to suppress wheat
613 defence (Liu *et al.*, 2016). To understand the role of *TaE3UBQ* during *Z. tritici*
614 infection, we silenced the gene transcript using BSMV VIGS. Silencing of *TaE3UBQ*
615 resulted in increased *Z. tritici* symptoms. We speculate that ZtSSP2 binding to
616 *TaE3UBQ* suppresses the wheat ubiquitin system and PTI. There exists
617 accumulating evidence that E3 ubiquitin ligase is a central regulator of plant
618 immunity and signalling (Trujillo and Shirasu, 2010; Marino *et al.*, 2012). In rice, the
619 resistance gene *Xa21* (*Xanthomonas oryzae pv. oryzae* locus 21) was shown to
620 require a RING- E3 ubiquitin XA21 binding protein 3 (XB3) which plays a key role in
621 accumulation of the XA21 protein and Xa21 mediated disease resistance (Wang *et al.*,
622 2006). In *Arabidopsis*, the Plant U-Box 12 (PUB12); a U-box E3 ligase is involved
623 in the PTI response against bacterial flagellin through Flagellin sensing 2 (FLS2) (Lu
624 *et al.*, 2011). Similarly, *Arabidopsis* *Tóxicos en Levadura* (ATL) family of RING finger
625 E3 ligase (ATL9) is induced by fungal chitin and is involved in resistance against the
626 biotrophic fungal pathogen, *Golovinomyces cichoracearum* (Deng *et al.*, 2017).

627 In conclusion, the ZtSSP-TaE3UBQ interaction may modulate and compromise
628 E3UBQ ligase activity suppressing wheat PTI. Virus-mediated gene silencing of
629 TaE3UBQ was found to promote STB susceptibility which agrees with TaE3UBQ
630 being a positive regulator of PTI. However, further work is needed to explore the
631 outcome of ZtSSP2 interaction on TaE3UBQ activity and to identify downstream host
632 interactors of TaE3UBQ which will provide information on how TaE3UBQ might
633 regulate immunity in wheat.

634

635

636

637

638

639

640

641

642

643

644

645

646

647

648

649

650

651

652

653

654

655

656

657

658

659

660 **Supporting Information**

661

662 **Fig. S1** *In silico* selection of non-annotated small secreted proteins (ZtSSP) of *Z.*
663 *tritici*. (a) Selection of small proteins, 492 proteins encoded by the *Z. tritici* genome
664 with EST support (do Amaral et al., 2012). (b) Proteins were classified based on their
665 size and proteins with 50-315 amino acid length were selected. (c) Numbers of
666 cysteine residues in the selected mature proteins after removing signal peptide. (d)
667 Proteins were annotated based on the presence of conserved functional domain.

668

669 **Fig. S2** BSMV mediated gene silencing (VIGS) of *phytoene desaturase (PDS)* gene
670 in wheat. Image of bleached PDS silenced fourth leaf at 10-14 days post inoculation
671 with BSMV.

672

673 **Fig. S3** Three homologues of *TaE3UBQ* are of high similarity. a) Nucleotide
674 sequence alignments and (b) Amino acid sequences of three homologues of
675 *TaE3UBQ* gene were obtained from Ensembl plant database. The three homologues
676 are located on chromosomes 1A, 1B and 1D, respectively, base variations indicated
677 with blue. The sequence alignment was performed using *MultAlin* (Corpet, 1998).
678 Regions targeted by VIGS1 and VIGS2 constructs are highlighted below by a solid
679 blue and green line respectively. Region targeted by conserved qPCR primers are
680 shown by black arrows.

681

682 **Fig. S4** Yeast two hybrid assay to test the interaction of RcSSP2 with Hve3UBQ.
683 Yeast transformed with Hve3UBQ, Hve3UBQ₁₂₆₋₂₁₉ and RcSSP2 cloned in the Gal4
684 bait and prey vectors. Yeast were grown for 4-5 days under selective Trp/Leu/His
685 drop out medium in presence of 0.3mM 3-amino-1,2,4-triazole (3-AT) and X- α -gal
686 medium or a non-selective Trp/Leu drop out medium (-TL) conditions. BD represents
687 Binding domain & AD, activating domain. Experiment was repeated three times
688 independently with three replicates per independent experiment.

689

690 **Fig. S5** *TaE3UBQ* protein topology illustration using MemBrain 3.1 (Yin *et al.*, 2017).
691 The protein sequence of *TaE3UBQ* shows transmembrane helix domains, an
692 extracellular loop (155-218) and intracellular regions within the protein structure. The
693 C3H2C3-ring is shown.

694

695 **Fig. S6** Expression profiles of wheat E3 ubiquitin ligase homeologs during *Z. tritici*
696 infection. Normalised expression data (in transcript per million (TPM)) retrieved from
697 expVIP (Borrill *et al.*, 2016) for all three *TaE3UBQ* homeologs following *Z. tritici*
698 infection and mock treatment at 1, 4, 9, 14 and 21 days post inoculation (dpi).

699

700

701

702

703

704

705

706

707

708 **Table S1.** List of putative candidate effector proteins of *Z. tritici* (ZtSSPs). Gene ID
709 corresponds to JGI gene ID, Gene annotations were obtained from JGI database
710 and blast search performed with NCBI BlastP. Functional annotation was performed
711 using NCBI CDD database. EffectorP 1.0 and ApoplasticP 1.0 was used to predict if
712 small, secreted proteins are predicted effectors and their localisation respectively: '+'
713 and '-' indicates positive and negative prediction. Candidates that matched Kettles *et*
714 *al.*, 2017 are referred as Zt.

715
716 **Table S2.** *Z. tritici* small, secreted proteins have potential homologues in other plant
717 pathogens. 46 out of 90 ZtSSP's show homologues in other plant pathogens. JGI
718 code, description, accession numbers, percentage identity and e-value. Cut-off of
719 50% percentage similarity and e-value 0.01 using NCBI Blast.

720
721 **Table S3.** Expression of seventeen conserved effector candidates across three *Z.*
722 *tritici* isolates IPO323, 553.11 and 560.11 at 7 dpi. The Logarithmic Fold Changes is
723 shown for each gene (LogFC), False Discovery Rate (FDR), FKPM values
724 Fragments Per Kilobase Million (FKM) and Filtered Reads (genes with a total read
725 count of <1 were filtered out of the analysis).

726
727 **Table S4.** List of primers used in this study.

728
729 **Table S5.** ZtSSP2 homologues in the Dothideomycetes with species, accession
730 numbers, description, e-value, sequence, and length of the 20 closest homologues
731 using NCBI BlastP. Red indicates signal peptide.

732
733 **Table S6.** List of wheat proteins identified as a potential interactors with *Z. tritici*
734 candidate ZtSSP2. Sequences obtained from positive clones in yeast 2 hybrid assay
735 was blasted against Ensemble wheat (TGACv1) dataset and corresponding full-
736 length sequences were obtained.

737
738 **Table S7.** *Z. tritici* small, secreted proteins with potential homologues only in present
739 in *Zymoseptoria brevis*. JGI code, description, accession numbers, percentage
740 identity and e-value. Cut-off of 50% percentage similarity and e-value 0.01 using
741 NCBI Blast.

742
743
744
745
746
747
748
749
750
751
752
753
754
755
756

757 **Data availability**

758 All data supporting the findings of this study are available within the paper and within
759 its supplementary materials published online.

760

761 **Acknowledgements**

762 This work was funded by the European Union's Horizon 2020 research and
763 innovation programme under the Marie Skłodowska-Curie grant agreement No.
764 674964 (CerealPath), SFI Career Development Award (15/CDA/3451), SFI Strategic
765 Partnerships Programme (16/SPP/3296), Irish Department of Agriculture, Food and
766 the Marine Research (DAFM) Stimulus Project VICCI (14/S/819) and Science
767 Foundation Ireland PI project 14/1A/2508. We would like to thank Dr. Eleanor Gilroy
768 (James Hutton Institute) for providing us Inf-1 and GV3101 and Dr. Stephen Kildea
769 (Teagasc, Carlow) for providing the 553.11 and 560.11 isolate.

770 **Author contributions**

771 S.J.K, F.D, P.S and A.F designed the experiments. S.J.K., A.R., D.D., M.M., B.Z.
772 performed the experiments. S.J.K., A.R., analysed the data. S.J.K and A.F wrote the
773 manuscript with input from D.D., P.S., J. B, F.D.

774

775

776

777

778

779

780

781

782

783

REFERENCES

- Anders S, Pyl PT, Huber W.** 2015. HTSeq: A Python framework to work with high-throughput sequencing data, *Bioinformatics*, **31**(2), 166-169
- Andrews, S.** 2010. FastQC: a quality control tool for high throughput sequence data.
- Armaleo D, Müller O, Lutzon, F, Andrésón ÓS, Blanc G, Bode HB, ... & BB Xavier.** 2019. The lichen symbiosis re-viewed through the genomes of *Cladonia grayi* and its algal partner *Asterochloris glomerata*. *BMC genomics*, **20**(1), 605.
- Bolger AM, Lohse M, Usadel B.** 2014. Trimmomatic: a flexible trimmer for Illumina sequence data. *Bioinformatics*, **30**(15): 2114-2120.
- Borrill, P, Ramirez-Gonzalez, R. and Uauy, C.** 2016. expVIP: a customizable RNA-seq data analysis and visualization platform. *Plant physiology*, **170** (4): 2172-2186.
- Bos JIB, Armstrong MR, Gilroy EM, Boevink PC, Hein I, Taylor RM, Zhendong T, Engelhardt S, Vetukuri RR, Harrower B.** 2010. *Phytophthora infestans* effector AVR3a is essential for virulence and manipulates plant immunity by stabilizing host E3 ligase CMPG1. *Proceedings of the National Academy of Sciences, USA* **107**, 9909–9914.
- Brading, PA, Verstappen EC, Kema GH, Brown JK.** 2002. A gene-for-gene relationship between wheat and *Mycosphaerella graminicola*, the *Septoria tritici* blotch pathogen. *Phytopathology*, **92**(4): 439-445.
- Brady NC.** 1983. *Advances in agronomy* (Vol. 36). Academic Press.
- Brennan, CJ, Zhou B, Benbow HR, Ajaz S, Karki SJ, Hehir JG, O'driscoll A, Feechan A, Mullins E. and Doohan FM.** 2020. Taxonomically restricted wheat genes interact with small secreted fungal proteins and enhance resistance to *Septoria tritici* blotch disease. *Frontiers in Plant Science*, 11, p.433.
- Chen S, Songkumarn P, Venu RC, Gowda M, Bellizzi M, Hu J, Liu W, Ebbole D, Meyers B, Mitchell T, Wang GL.** 2013. Identification and characterization of in planta-expressed secreted effector proteins from *Magnaporthe oryzae* that induce cell death in rice. *Molecular plant-microbe interactions*, **26**(2): 191-202.
- Corpet, F.** 1988. Multiple sequence alignment with hierarchical clustering. *Nucleic acids research*, **16**(22), pp.10881-10890.
- de Hoog G.S, Mayser P, Haase G, Horr  R, Horrevorts, A.M.** 2000. A new species, *Phialophora europaea*, causing superficial infections in humans. *Mycoses*, **43**(11-12), p.409.
- Deng F, Guo T, Lefebvre M, Scaglione S, Antico CJ, Jing T, Yang X, Shan W, Ramonell KM.** 2017. Expression and regulation of ATL9, an E3 ubiquitin ligase involved in plant defense. *PloS one*, **12**(11), p.e0188458.
- Deslandes L, Rivas S.** 2012. Catch me if you can: bacterial effectors and plant targets. *Trends in plant science*. **17**(11): 644-655.

do Amaral AM, Antoniw J, Rudd JJ and Hammond-Kosack KE. 2012. Defining the predicted protein secretome of the fungal wheat leaf pathogen *Mycosphaerella graminicola*. *PLoS One*, **7**(12), p.e49904.

Dou D, Zhou JM. 2012. Phytopathogen effectors subverting host immunity: different foes, similar battleground. *Cell host & microbe*. **12**(4): 484-495.

Douchkov D, Nowara D, Zierold U, Schweizer P. 2005. A high-throughput gene-silencing system for the functional assessment of defense-related genes in barley epidermal cells. *Molecular Plant-Microbe Interactions*, **18**(8), 755-761.

Earley KW, Haag JR, Pontes O, Opper K, Juehne T, Song K, Pikaard CS. 2006. Gateway-compatible vectors for plant functional genomics and proteomics. *The Plant Journal*, **45**(4), 616-629.

Eyal Z, Scharen AL, Huffman MD, Prescott JM. 1985. Global insights into virulence frequencies of *Mycosphaerella graminicola*. *Phytopathology*, **75**(12), 1456-1462.

Fernandez-Pozo N, Rosli HG, Martin GB, Mueller LA. 2015. The SGN VIGS tool: user-friendly software to design virus-induced gene silencing (VIGS) constructs for functional genomics. *Molecular plant*, **8**(3), 486-488.

Fones H, Gurr S. 2015. The impact of Septoria tritici Blotch disease on wheat: An EU perspective. *Fungal Genetics and Biology*, **79**, 3-7.

Fones, H.N., Eyles, C.J., Kay, W., Cowper, J. and Gurr, S.J., 2017. A role for random, humidity-dependent epiphytic growth prior to invasion of wheat by *Zymoseptoria tritici*. *Fungal Genetics and Biology*, **106**, pp.51-60.

Franco-Orozco B, Berepiki A, Ruiz O, Gamble L, Griffe LL, Wang S, Birch PR, Kanyuka K, Avrova A. 2017. A new proteinaceous pathogen-associated molecular pattern (PAMP) identified in Ascomycete fungi induces cell death in Solanaceae. *New Phytologist*, **214**(4), 1657-1672.

Gehl C, Waadt R, Kudla J, Mendel RR, Hänsch R. 2009. New GATEWAY vectors for high throughput analyses of protein-protein interactions by bimolecular fluorescence complementation. *Molecular plant*, **2**(5), 1051-1058.

Goodwin, S.B., M'barek, S.B., Dhillon, B., Wittenberg, A.H., Crane, C.F., Hane, J.K. Foster, A.J., Van der Lee, T.A., Grimwood, J., Aerts, A. and Antoniw, J. 2011. Finished genome of the fungal wheat pathogen *Mycosphaerella graminicola* reveals dispensome structure, chromosome plasticity, and stealth pathogenesis. *PLoS Genet*, **7**(6), p.e1002070.

Hogenhout SA, Van der Hoorn RA, Terauchi R, Kamoun S. 2009. Emerging concepts in effector biology of plant-associated organisms. *Molecular plant-microbe interactions*, **22**(2), 115-122.

Holzberg S, Brosio P, Gross C, Pogue GP. 2002. Barley stripe mosaic virus-induced gene silencing in a monocot plant. *The Plant Journal*, **30**(3), 315-327.

- Jones JD, Dangl JL.** 2006. The plant immune system. *Nature*, **444**(7117): 323-329.
- Kema GH, Gohari AM, Aouini L, Gibriel HA, Ware SB, van Den Bosch F, Manning-Smith R, Alonso-Chavez V, Helps J, M'Barek SB, Mehrabi R.** 2018. Stress and sexual reproduction affect the dynamics of the wheat pathogen effector AvrStb6 and strobilurin resistance. *Nature genetics*, **50**(3), 375.
- Kema GH, van Silfhout CH.** 1997. Genetic variation for virulence and resistance in the wheat-*Mycosphaerella graminicola* pathosystem III. Comparative seedling and adult plant experiments. *Phytopathology*, **87**(3), 266-272.
- Kettles GJ, Bayon C, Canning G, Rudd JJ, Kanyuka K.** 2017. Apoplastic recognition of multiple candidate effectors from the wheat pathogen *Zymoseptoria tritici* in the nonhost plant *Nicotiana benthamiana*. *New Phytologist*, **213**(1), 338-350.
- Kettles GJ, Bayon C, Sparks CA, Canning G, Kanyuka K, Rudd JJ.** 2018. Characterization of an antimicrobial and phytotoxic ribonuclease secreted by the fungal wheat pathogen *Zymoseptoria tritici*. *New Phytologist*, **217**(1), 320-331.
- Kim D, Pertea G, Trapnell C, Pimentel H, Kelley R, Salzberg SL.** 2013. TopHat2: accurate alignment of transcriptomes in the presence of insertions, deletions and gene fusions. *Genome Biology*, **14**, R36.
- Kumar S, Stecher G, Tamura, K.** 2016. MEGA7: molecular evolutionary genetics analysis version 7.0 for bigger datasets. *Molecular biology and evolution*, **33**(7), 1870-1874.
- Lee WS, Rudd JJ, Hammond-Kosack KE, Kanyuka K.** 2014. *Mycosphaerella graminicola* LysM effector-mediated stealth pathogenesis subverts recognition through both CERK1 and CEBiP homologues in wheat. *Molecular Plant-Microbe Interactions*, **27**(3), 236-243.
- Li H, Handsaker B, Wysoker A, Fennell T, Ruan J, Homer N, Marth G, Abecasis G, Durbin R. and 1000 Genome Project Data Processing Subgroup.** 2009. The Sequence alignment/map (SAM) format and SAMtools. *Bioinformatics*, **25**, 2078-2079.
- Liu C, Pedersen C, Schultz-Larsen T, Aguilar GB, Madriz-Ordeñana K, Hovmøller MS, Thordal-Christensen H.** 2016. The stripe rust fungal effector PEC 6 suppresses pattern-triggered immunity in a host species-independent manner and interacts with adenosine kinases. *New Phytologist*.
- Livak KJ, Schmittgen TD.** 2001. Analysis of relative gene expression data using real-time quantitative PCR and the 2⁻ΔΔCT method. *methods*, **25**(4), 402-408.
- Lu D, Lin W, Gao X, Wu S, Cheng C, Avila J, Heese A, Devarenne TP, He P, Shan L.** 2011. Direct ubiquitination of pattern recognition receptor FLS2 attenuates plant innate immunity. *Science*, **332**(6036), 1439-1442.
- Lynch KM, Zannini E, Guo J, Axel C, Arendt EK, Kildea S, Coffey A.** 2016. Control of *Zymoseptoria tritici* cause of septoria tritici blotch of wheat using antifungal *Lactobacillus* strains. *Journal of applied microbiology*, **121**(2), 485-494.

- M'Barek SB, Cordewener JH, Ghaffary SMT, van der Lee TA, Liu Z, Gohari AM, Mehrabi R, America AH, Robert O, Friesen TL, Hamza S.** 2015. FPLC and liquid-chromatography mass spectrometry identify candidate necrosis-inducing proteins from culture filtrates of the fungal wheat pathogen *Zymoseptoria tritici*. *Fungal Genetics and Biology*, **79**, 54-62.
- Marchler-Bauer A, Lu S, Anderson JB, Chitsaz F, Derbyshire MK, DeWeese-Scott C, Fong JH, Geer LY, Geer RC, Gonzales NR, Gwadz M.** 2010. CDD: a Conserved Domain Database for the functional annotation of proteins. *Nucleic acids research*, **39**(suppl_1), D225-D229.
- Marino D, Peeters N, Rivas S.** 2012. Ubiquitination during plant immune signaling. *Plant physiology*, **160**(1): 15-27.
- Marshall R, Kombrink A, Motteram J, Loza-Reyes E, Lucas J, Hammond-Kosack KE, Thomma BP, Rudd JJ.** 2011. Analysis of two in planta expressed LysM effector homologues from the fungus *Mycosphaerella graminicola* reveals novel functional properties and varying contributions to virulence on wheat. *Plant physiology*, **156**(2), 756-769.
- McLellan, H., Chen, K., He, Q., Wu, X., Boevink, P.C., Tian, Z. and Birch, P.R.** 2020. The ubiquitin E3 ligase PUB17 positively regulates immunity by targeting a negative regulator, KH17, for degradation. *Plant Communications*, p.100020.
- Meile L, Croll D, Brunner PC, Plissonneau C, Hartmann FE, McDonald BA, Sánchez-Vallet A.** 2018. A fungal avirulence factor encoded in a highly plastic genomic region triggers partial resistance to septoria tritici blotch. *New Phytologist*, **219**(3), 1048-1061.
- Mirzadi Gohari A, Ware SB, Wittenberg AH, Mehrabi R, Ben M'Barek S, Verstappen EC, van der Lee TA, Robert O, Schouten H.J. de Wit PP, Kema GH.** 2015. Effector discovery in the fungal wheat pathogen *Zymoseptoria tritici*. *Molecular plant pathology*, **16**(9), 931-945.
- Motteram J, Küfner I, Deller S, Brunner F, Hammond-Kosack KE, Nürnberger T, Rudd JJ.** 2009. Molecular characterization and functional analysis of MgNLP, the sole NPP1 domain-containing protein, from the fungal wheat leaf pathogen *Mycosphaerella graminicola*. *Molecular Plant-Microbe Interactions*, **22**(7), 790-799.
- Mukhtar MS, Carvunis AR, Dreze M, Epple P, Steinbrenner J, Moore J, Tasan M, Galli M, Hao T, Nishimura MT, Pevzner SJ.** 2011. Independently evolved virulence effectors converge onto hubs in a plant immune system network. *science*, **333**(6042): 596-601.
- Nakagawa T, Kurose T, Hino T, Tanaka K, Kawamukai M, Niwa Y, Toyooka K, Matsuoka K, Jinbo T, Kimura T.** 2007. Development of series of gateway binary vectors, pGWBs, for realizing efficient construction of fusion genes for plant transformation. *Journal of bioscience and bioengineering*, **104**(1), 34-41.

- Nelson BK, Cai X, Nebenführ A.** 2007. A multicolored set of in vivo organelle markers for co-localization studies in Arabidopsis and other plants. *The Plant Journal*, **51**(6), 1126-1136.
- Nielsen, H.** 2017. Predicting secretory proteins with SignalP. In *Protein function prediction* pp. 59-73. Humana Press, New York, NY.
- Park CH, Chen S, Shirsekar G, Zhou B, Khang CH, Songkumarn P, Afzal AJ, Ning Y, Wang R, Bellizzi M, Valent B.** 2012. The *Magnaporthe oryzae* effector AvrPiz-t targets the RING E3 Ubiquitin Ligase APIP6 to suppress pathogen-associated molecular pattern-triggered immunity in rice. *The Plant Cell*, **24** (11): 4748-4762.
- Park, C.H., Shirsekar, G., Bellizzi, M., Chen, S., Songkumarn, P., Xie, X., Shi, X., Ning, Y., Zhou, B., Suttiviriya, P. and Wang, M.** 2016. The E3 ligase APIP10 connects the effector AvrPiz-t to the NLR receptor Piz-t in rice. *PLoS pathogens*, **12** (3), p.e1005529.
- Perochon A, Dieterle S, Pouzet C, Aldon D, Galaud JP, Ranty B.** 2010. Interaction of a plant pseudo-response regulator with a calmodulin-like protein. *Biochemical and biophysical research communications*, **398**(4), 747-751.
- Pliego C, Nowara D, Bonciani G, Gheorghe DM, Xu R, Surana P, Whigham E, Nettleton D, Bogdanove AJ, Wise RP, Schweizer P.** 2013. Host-induced gene silencing in barley powdery mildew reveals a class of ribonuclease-like effectors. *Molecular Plant-Microbe Interactions*, **26**(6), 633-642.
- Queiróz A.J, Pereira Domingos F, Antônio J.R,** 2018. Chromoblastomycosis: clinical experience and review of literature. *International journal of dermatology*, **57**(11), pp.1351-1355.
- R Core Team.** 2016. R: a language and environment for statistical computing. Vienna, Austria: R Foundation for statistical Computing. <https://www.R-project.org/>
- Rafiqi M, Jelonek L, Akum NF, Zhang F, Kogel KH.** 2013. Effector candidates in the secretome of *Piriformospora indica*, a ubiquitous plant-associated fungus. *Frontiers in plant science*, **4**,228.
- Robinson MD, Oshlack A.** 2010. A scaling normalization method for differential expression analysis of RNA-seq data. *Genome Biology*, **11**, R25.
- Robinson MD, Smyth GK.** 2008. Small sample estimation of negative binomial dispersion, with applications to SAGE data. *Biostatistics*, **9**, 321-332.
- Rudd JJ, Kanyuka K, Hassani-Pak K, Derbyshire M, Andongabo A, Devonshire J, Lysenko A, Saqi M, Desai NM, Powers SJ, Hooper J.** 2015. Transcriptome and metabolite profiling of the infection cycle of *Zymoseptoria tritici* on wheat reveals a biphasic interaction with plant immunity involving differential pathogen chromosomal contributions and a variation on the hemibiotrophic lifestyle definition. *Plant physiology*, **167**(3), 1158-1185.

- Sánchez-Vallet, A., McDonald, M.C., Solomon, P.S. and McDonald, B.A.** 2015. Is *Zymoseptoria tritici* a hemibiotroph? *Fungal Genetics and Biology*, **79**, 29-32.
- Schweizer P, Pokorny J, Schulze-Lefert P, Dudler R.** 2000. Double-stranded RNA interferes with gene function at the single-cell level in cereals. *The Plant Journal*, **24**(6), 895-903.
- Scofield SR, Huang L, Brandt AS, Gill BS.** 2005. Development of a virus-induced gene-silencing system for hexaploid wheat and its use in functional analysis of the Lr21-mediated leaf rust resistance pathway. *Plant Physiology*, **138**(4), 2165-2173.
- Shetty, N.P., Kristensen, B.K., Newman, M.A., Møller, K., Gregersen, P.L. and Jørgensen, H.L.** 2003. Association of hydrogen peroxide with restriction of *Septoria tritici* in resistant wheat. *Physiological and Molecular Plant Pathology*, **62**(6), pp.333-346.
- Sperschneider J, Dodds PN, Singh KB, Taylor JM.** 2018. ApoplastP: prediction of effectors and plant proteins in the apoplast using machine learning. *New Phytologist*, **217**(4), 1764-1778.
- Sperschneider J, Gardiner DM, Dodds PN, Tini F, Covarelli L, Singh KB, Manners JM, Taylor JM.** 2016. EffectorP: predicting fungal effector proteins from secretomes using machine learning. *New Phytologist*, **210**(2), 743-761.
- Stergiopoulos I, de Wit PJ.** 2009. Fungal effector proteins. *Annual review of phytopathology*. **47**: 233-263.
- Trapnell C, Williams BA, Pertea G, Mortazavi A, Kwan G, van Baren MJ, Salzberg SL, Wold BJ, Pachter L.** 2010. Transcript assembly and quantification by RNA-Seq reveals unannotated transcripts and isoform switching during cell differentiation. *Natural Biotechnology*, **28**, 511-515.
- Trujillo M, Shirasu K.** 2010. Ubiquitination in plant immunity. *Current Opinion in Plant Biology* **13**: 402–408
- Üstün S, Sheikh A, Gimenez-Ibanez S, Jones AM, Ntoukakis V, Börnke F.** 2016. The proteasome acts as a hub for plant immunity and is targeted by *Pseudomonas* type-III effectors. *Plant physiology*, pp.-00808.
- Van Wijk SJ, De Vries SJ, Kemmeren P, Huang A, Boelens R, Bonvin AM, Timmers HTM.** 2009. A comprehensive framework of E2–RING E3 interactions of the human ubiquitin–proteasome system. *Molecular systems biology*, **5**(1).
- Váry Z, Mullins E, McElwain JC, Doohan, FM.** 2015. The severity of wheat diseases increases when plants and pathogens are acclimatized to elevated carbon dioxide. *Global change biology*, **21**(7), 2661-2669.
- Wang YS, Pi LY, Chen X, Chakrabarty PK, Jiang J, De Leon AL, Liu GZ, Li L, Benny U, Oard J, Ronald PC.** 2006. Rice XA21 binding protein 3 is an ubiquitin ligase required for full Xa21-mediated disease resistance. *The Plant Cell*, **18**(12):3635-3646.

Yin X, Yang J, Xiao F, Yang Y, Shen, H.B. 2018. MemBrain: an easy-to-use online webserver for transmembrane protein structure prediction. *Nano-micro letters*, **10**(1), 2.

Zhong Z, Marcel TC, Hartmann FE, Ma X, Plissonneau C, Zala M, Ducasse A, Confais J, Compain J, Lapalu N, Amselem J. 2017. A small secreted protein in *Zymoseptoria tritici* is responsible for avirulence on wheat cultivars carrying the Stb6 resistance gene. *New Phytologist*, **214**(2), 619-631.

Zhou B, Benbow HR, Brennan CJ, Arunachalam C, Karki SJ., Mullins E, Feechan A, Burke JI, Doohan FM. 2020. Wheat Encodes Small, Secreted Proteins That Contribute to Resistance to Septoria Tritici Blotch. *Frontiers in Genetics*, **11**, 469.

784 **Figure Legends**

785

786 **Fig. 1.** ZtSSP2 is a secreted protein. (a) Design of the gateway compatible yeast
787 pGADT7-ZtSSP2-Suc2 vector and Invertase mutant yeast strain SEY6210 used for
788 the secretion assay (Brennan *et al.*, 2020). (b) Yeast strain carrying *ZtSSP2* with
789 secretion signal fused in frame with the Invertase gene *Suc2* were able to grow in
790 sucrose containing drop out media (SD-TL) sucrose therefore cells will grow if
791 Invertase is secreted. SEY6210 carrying pGAD- Δ SP:SUC2²²⁻⁵¹¹² vector was used as
792 negative control while SEY6210 with pGAD-SUC2^{Full length} acts as positive control.
793 This experiment was repeated three times independently with three replicates per
794 independent experiment.

795

796

797 **Fig. 2.** ZtSSP2 (*Z. tritici* small, secreted protein candidate 2) homologues are widely
798 present across Dothideomycetes. (a) Protein alignment using ClustalW, of the full
799 protein sequence of *Z. tritici* ZtSSP2 with homologues from seven plant infecting
800 Dothideomycetes fungi. Asterisk indicates conserved cysteine residues and shading
801 represents identical or similar amino acids. Signal peptide predicted using SignalP
802 4.1 (indicated by red line) (b) The Unrooted maximum likelihood phylogeny of
803 ZtSSP2 and the 20 closest orthologues including plant pathogens (green), other non-
804 pathogenic Dothideomycetes (orange) and Eurotiomycetes (blue) which are human
805 pathogens. Tree was generated with MEGA7 (Kumar *et al.* 2016), Bootstrap values
806 are based on 1000 replications. Sequences were obtained by blastp (NCBI) and
807 aligned using ClustalW.

808

809 **Fig. 3.** *ZtSSP2* is expressed at different stages of *Z. tritici* infection (2-10 dpi
810 biotrophic and 14-21 dpi necrotrophic stage). Gene expression analysis of *ZtSSP2*
811 un-infected control, at 2, 4, 8, 10, 14, 21 dpi of wheat (cv.Remus) with *Z. tritici* isolate
812 560.11 (Lynch *et al.* 2016). Control plants were inoculated with Tween 20. RNA was
813 extracted from three wheat leaves per time point followed by reverse transcription
814 into cDNA. The qPCR was performed on cDNA using specific primers for *ZtSSP2*.
815 The expression levels of β -*tubulin* (*Z. tritici*) were used to normalize the expression
816 levels of *ZtSSP2*. Each independent experiment had three leaves each from three
817 individual plants. The bars represent the mean relative expression \pm SEM of three
818 independently replicated experiments. Different letters above bars indicate significant
819 differences, as determined by Tukey's test (* $P < 0.05$).

820

821 **Fig. 4** Single cell death assay in wheat leaves. Wheat leaves cv. Kanzler were co-
822 bombarded with pUbiGus as a transformation marker, pEG101 for overexpression of
823 *ZtSSP2* (PEG101:*ZtSSP2*), and the *B-Peru/C1-expression* plasmid pBC17 that
824 induces anthocyanin accumulation in wheat epidermal cells. **(a)** Unstained wheat
825 leaf showing epidermal cells that accumulate anthocyanin (arrow; bar=20 μ m) 4 days
826 after bombardment and **(b)** β -glucuronidase (GUS) expressing cells after GUS
827 staining. **(c)** Quantification of the relative number of anthocyanin producing cells
828 calculated as the ratio of anthocyanin accumulated cells to the number of GUS
829 expressing cells. Co-transformation of pBC17 and pUbiGUS with the empty vector
830 pEG101 and pEG101: *Zt-6* served as a positive control inducing cell death. Values

831 are the means of four independent experiments with 7 leaves counted per repetition
832 (Bars \pm SEM). The asterisk on top of bar represents significant differences
833 determined by Tukey test (* for $P < 0.05$).

834

835 **Fig. 5** Interaction of (Δ SP) *ZtSSP2* with host protein *TaE3UBQ*. **(a)** Yeast two-hybrid
836 assay using the yeast cells transformed with *TaE3UBQ* and (Δ SP) *ZtSSP2* cloned in
837 the Gal4 bait (BD) and prey vectors (AD). Yeast strain Y2HGold co-expressing the
838 vector BD containing *TaE3UBQ*, *TaE3UBQ*₁₂₆₋₂₁₉, *TaSSP6* or empty bait vector (BD-
839 X) and the prey vector containing *ZtSSP2*, *Zt10*, *Zt06* or empty vector (AD-X) were
840 grown on auxotrophic media (SD/-Leu-Trp) (left panel) or selective Trp/Leu/His drop
841 out medium in presence of 0.5 mM 3-amino-1,2,4-triazole (3-AT). Only yeast cells
842 co-expressing *ZtSSP2* and *TaE3UBQ*₁₂₆₋₂₁₉ grew on selective media (SD/-Leu-Trp-
843 His) (middle panel) and showed α -galactosidase activity encoded by α -galactosidase
844 (MEL1) (right panel). BD-*TaSSP6* and AD-*Zt06* was used as positive control (Zhou
845 *et al.*, 2020). The experiment was repeated independently three times, three plates
846 per experiment with similar results. **(b)** Validation of *in planta* interaction of (Δ SP)
847 *ZtSSP2* with wheat Ubiquitin protein visualized by the bimolecular fluorescence
848 complementation (BiFC) assay. Confocal microscopy images of representative *N.*
849 *benthamiana* epidermal leaf cells expressing proteins fused to the N- or C-terminal
850 part of the YFP as indicated. YFP, brightfield are shown both separately and as an
851 overlay. Scale bar is 10 μ m. In both experiment a and b, candidate Zt-10 was used
852 as a negative control while Cnx6 homodimerisation was used as BiFC positive
853 control. Experiments were repeated at least two times independently with similar
854 results (three leaves each from individual plants). **(c)** Confirmation of the interaction
855 between *ZtSSP2* and *TaE3UBQ* by co-immunoprecipitation assays. Western blot of
856 total proteins from *N. benthamiana* leaves co-infiltrated with the construct and co-
857 immunoprecipitated using GFP-Trap magnetic beads. Expression of constructs in
858 the leaves is indicated by '+'. Immunoblots were performed using anti-GFP and anti-
859 HA antibodies. The protein size markers are indicated in kDa.

860

861 **Fig. 6** Sequence analysis of wheat E3 ubiquitin ligase, *T. aestivum* E3 UBQ ligase
862 protein (*TaE3UBQ*). **(a)** Schematic representation of the structure of *TaE3UBQ* and
863 the conserved RING finger motif using TMpred and CCD domain database. **(b)**
864 Sequence alignment of the C3H2C3-type RING finger conserved motif in *TaE3UBQ*
865 homologues in Barley (Gene Bank accession no. BAJ95361.1), Brachypodium
866 (XP_003568812.1), Oryzae (XP_015640584.1), Maize (PWZ17186.1), Arabidopsis
867 (NP_178156.1), Millet (RLM97696.1), Sorghum (XP_002439378.1). Putative Zn²⁺-
868 interacting amino acid residues are indicated by red while, conserved and non-
869 conserved residues are highlighted by black and white, respectively. **(c)** GFP-
870 *TaE3UBQ* fluorescent signal localises to the cell periphery similar to the signal
871 obtained from a plasma membrane marker pm-yk (Nelson *et al.*, 2007) in *N.*
872 *benthamiana* cells. The GFP fluorescent protein was found distributed throughout
873 the cell of transformed *N. benthamiana* leaf cells. Bars = 20 μ m

874

875 **Fig. 7** BSMV mediated virus induced gene silencing (VIGS) of wheat E3 ubiquitin
876 ligase (*TaE3UBQ*) resulted in increased *Z. tritici* susceptibility of wheat leaves.
877 Wheat leaves at the second leaf stage (cv. Longbow) were treated with either FES
878 (VIGS buffer), BSMV:00 (empty vector) or BSMV:UBQ_V1 or BSMV:UBQ_V2
879 (constructs targeting all three homeologs of *TaE3UBQ*). The third and fourth leaves
880 of VIGS treated plants were inoculated with either mock (Tween) or *Z. tritici* (560.11).
881 Subsequently, the third leaves were collected for gene expression studies and the
882 fourth leaves for phenotyping and spore count. (a) Relative transcript abundance of
883 all *TaE3UBQ* homeologs in knockdown plants (5-6 leaves each from individual
884 seedlings per treatment per replicate). (b, c) Phenotype of VIGS treated leaves
885 infected with *Z. tritici* at 21 days post inoculation (10 leaves each from individual
886 seedlings per treatment per replicate). (d) Average spore counts per ml were
887 counted over 2 cm leaf lengths (7 leaves each from individual seedlings per
888 treatment per replicate). Three independent experiments were carried out. Bars with
889 the same letter are not significantly different. ($P < 0.05$).

890

891

892

893

894

895

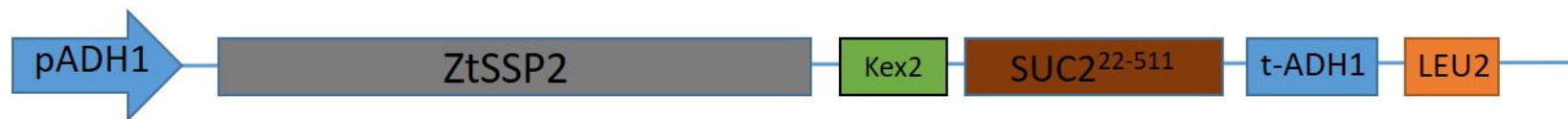
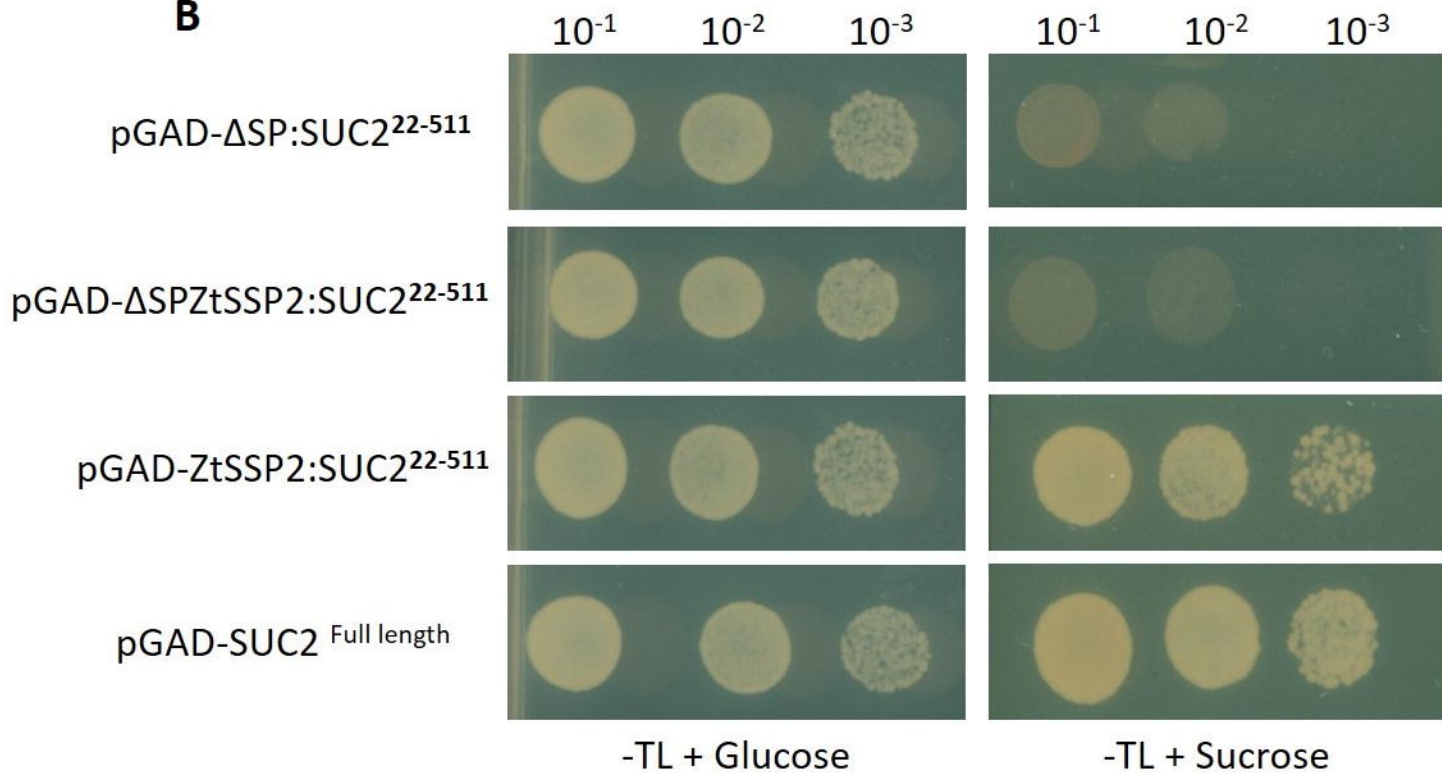
896

897

898

899

900

A**B**

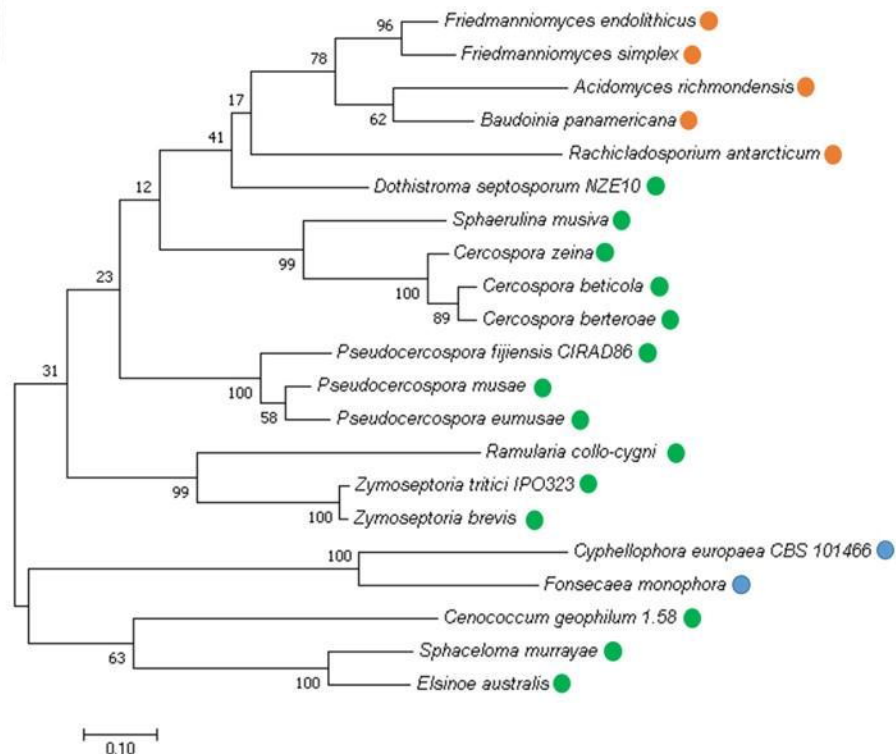
(a)



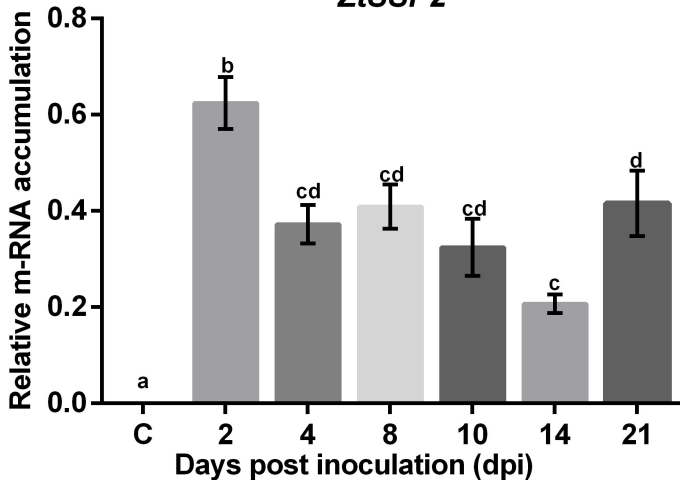
C. beticola 180 NYGTGILVTGLLAVFGLM
S. musiva 187 NYGTGIFALLGNAVEFLM
D. septosporum 181 NYGTGIFMAGLLAVFGFAL
M. eumusae 180 SYGTGIFVTGLLAVFGLAL
P. fijiensis 181 NYGTGIFVTGLLAVFGLAL
R. collo-cygni 194 AYGSIFFAAGLLIFGLAL
Z. tritici 181 SYGSGLAAGLLIFGLAL
Z. brevis 182 SYGSGLAAGLLIFGLAL

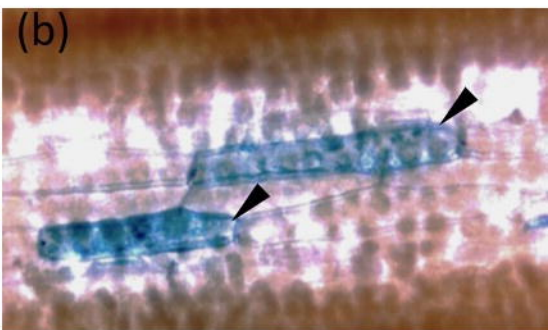
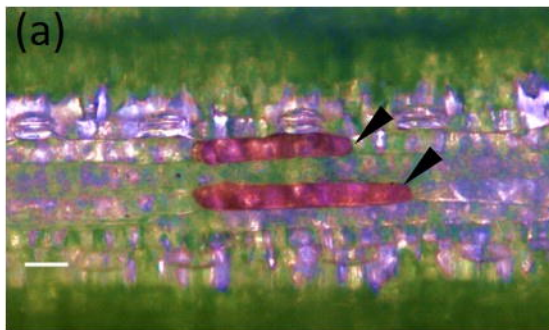
- Plant infecting Dothideomycetes;
Mycosphaerellaceae
- Other Dothideomycetes
- Eurotiomycetes

(b)

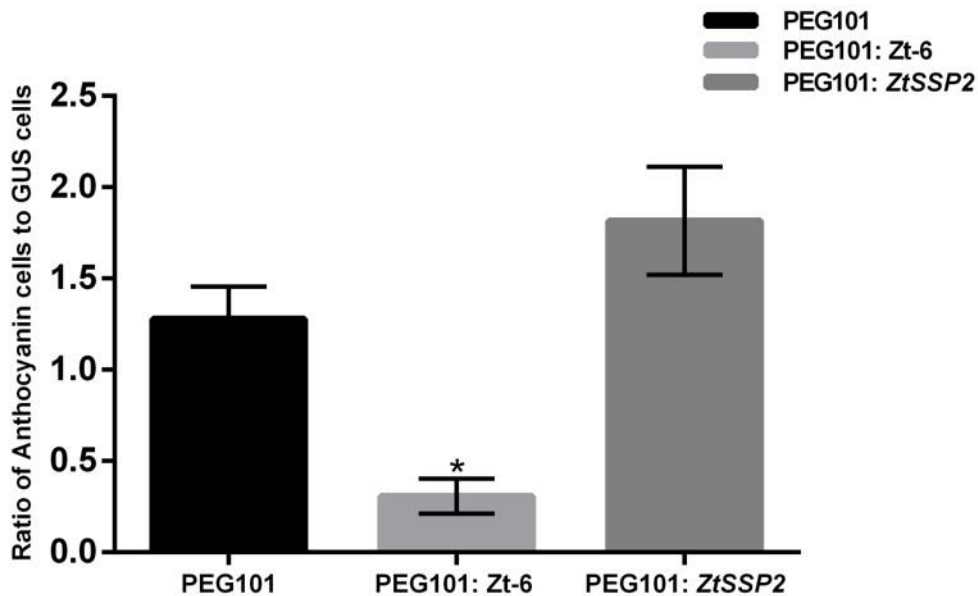


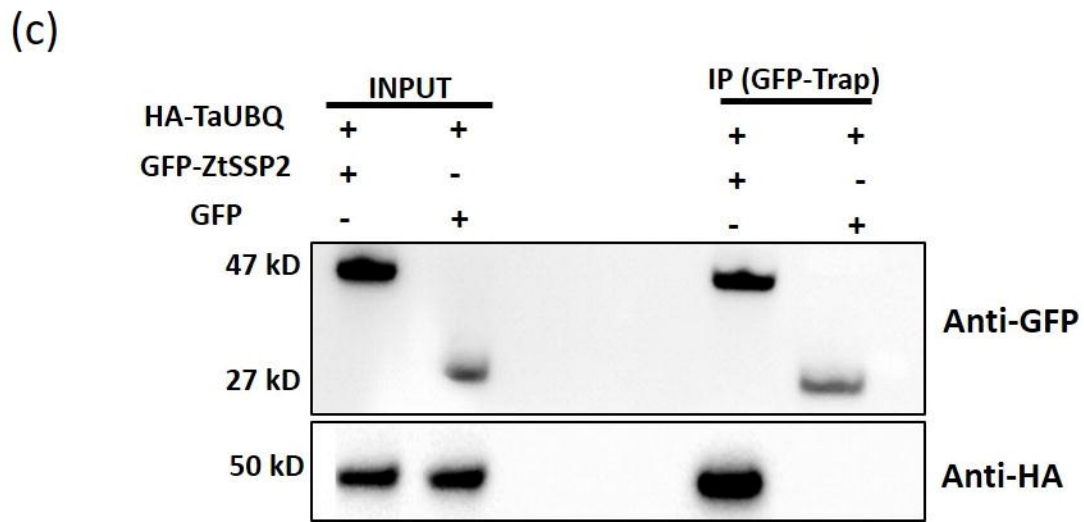
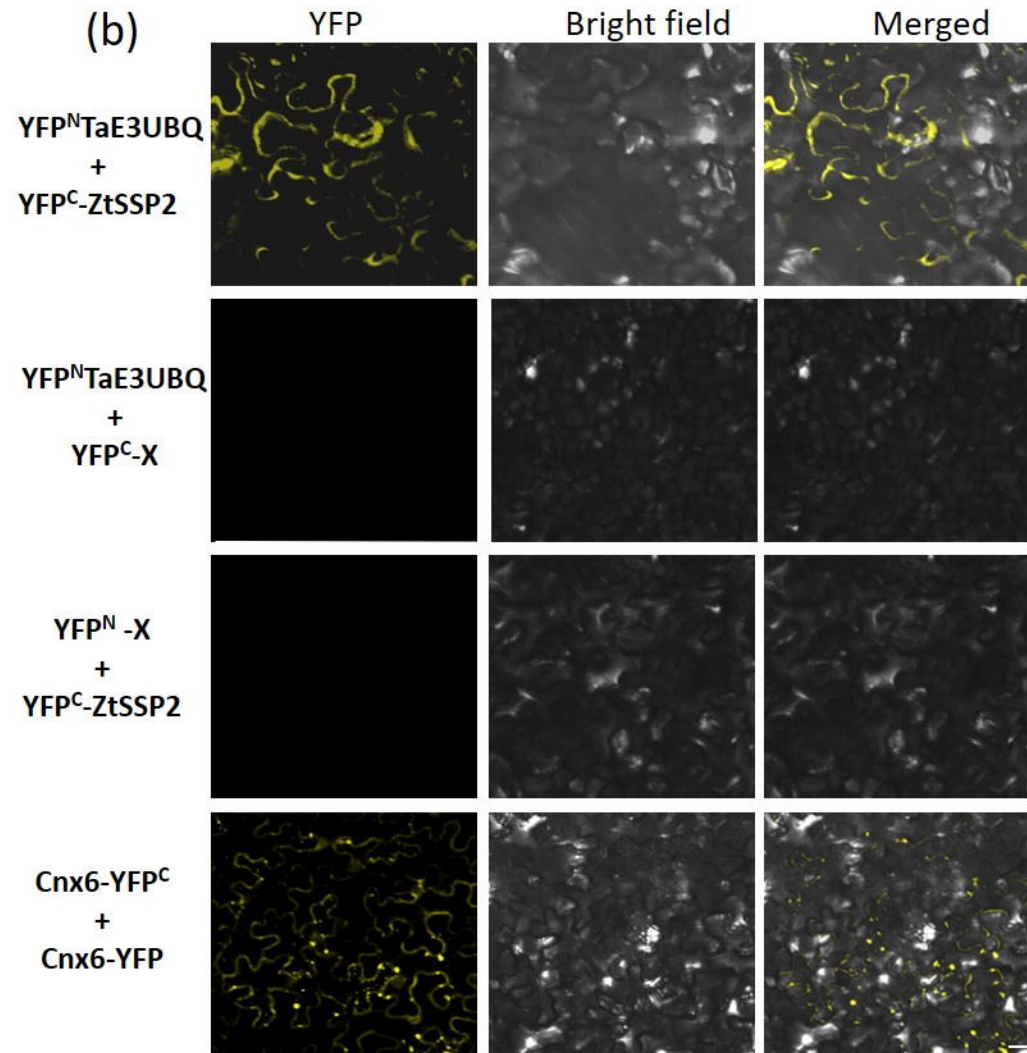
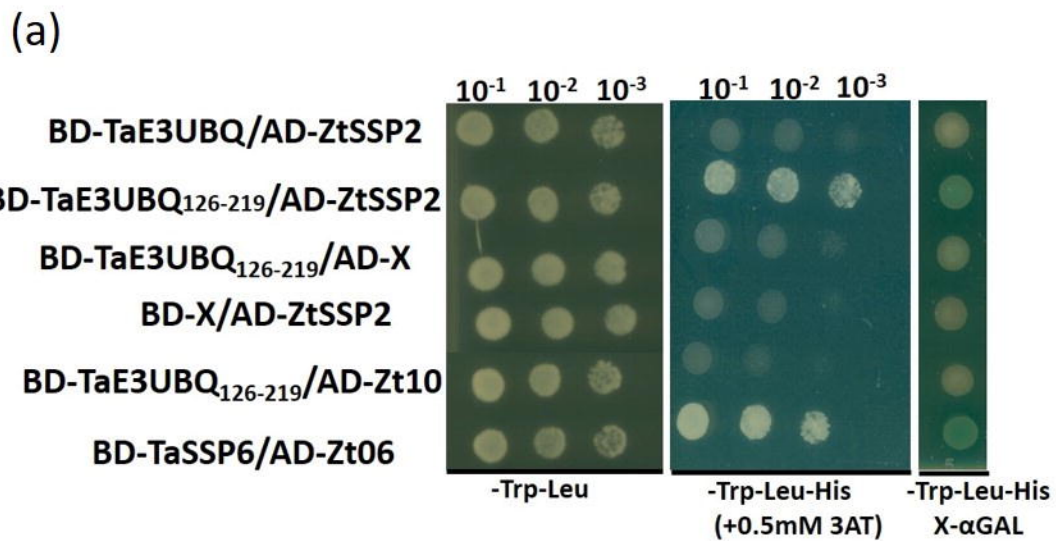
ZtSSP2

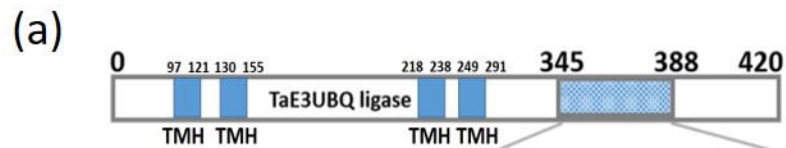




(c)







(b) Multiple sequence alignment of the C3H2C3-RING domain (residues 345-388) from various species. The alignment shows conserved residues in red and conserved motifs in black. The species listed are Wheat, Barley, Brachypodium, Oryzae, Maize, Arabidopsis, Millet, and Sorghum. The alignment starts at residue 1 for each species.

Species	Sequence
Wheat	1 C C I C L A R Y S N N D D L R E L P C T H F F H K E C V D K W L K I N A L C P L C K
Barley	1 C C I C L A R Y S N N D D L R E L P C T H F F H K E C V D K W L K I N A L C P L C K
Brachypodium	1 C C I C L A R Y V N N D D L R E L P C T H F F H K E C V D K W L K I N A L C P L C K
Oryzae	1 C C I C L A R Y V D N D D L R E L P C A H F F H K D C V D K W L K I N A L C P L C K
Maize	1 C C I C L A R Y V D N D D L R L L P C G H F F H K D C V D K W L K I N A L C P L C K
Arabidopsis	1 C C I C L T R Y G D D E Q V R E L P C S H V F H V D C V D K W L K I N A T C P L C K
Millet	1 C C I C L A R Y V D N D E L R L L P C G H F F H K D C V D K W L K I N A L C P L C K
Sorghum	1 C C I C L A R Y V D N D D L R L L P C G H F F H K D C V D K W L K I N A L C P L C K

